Kent Academic Repository

Ottolini, Christian S, Newnham, Louise J, Capalbo, Antonio, Natesan, Senthilkumar A, Joshi, Hrishikesh A, Cimadomo, Danilo, Griffin, Darren K., Sage, Karen, Summers, Michael C, Thornhill, Alan R and others (2015) *Genome-wide maps of recombination and chromosome segregation in human oocytes and embryos show selection for maternal recombination rates.* Nature Genetics, 47 (7). pp. 727-735. ISSN 1061-4036.

Downloaded from

https://kar.kent.ac.uk/59356/ The University of Kent's Academic Repository KAR

The version of record is available from

https://doi.org/10.1038/ng.3306

This document version

Author's Accepted Manuscript

DOI for this version

Licence for this version

UNSPECIFIED

Additional information

Versions of research works

Versions of Record

If this version is the version of record, it is the same as the published version available on the publisher's web site. Cite as the published version.

Author Accepted Manuscripts

If this document is identified as the Author Accepted Manuscript it is the version after peer review but before type setting, copy editing or publisher branding. Cite as Surname, Initial. (Year) 'Title of article'. To be published in *Title of Journal* , Volume and issue numbers [peer-reviewed accepted version]. Available at: DOI or URL (Accessed: date).

Enquiries

If you have questions about this document contact ResearchSupport@kent.ac.uk. Please include the URL of the record in KAR. If you believe that your, or a third party's rights have been compromised through this document please see our Take Down policy (available from https://www.kent.ac.uk/guides/kar-the-kent-academic-repository#policies).

"MeioMaps of genome-wide recombination and chromosome segregation in human oocytes and embryos reveal selection for maternal recombination rates".

Christian S. Ottolini[1,2*], Louise Newnham[3*], Antonio Capalbo[4*], Senthilkumar A. Natesan[5], Hrishikesh A. Joshi[5], Danilo Cimadomo[4], Darren K. Griffin[2], Karen Sage[1], Michael C. Summers[1,2], Alan R. Thornhill[5], Elizabeth Housworth[6], Alex D. Herbert[3], Laura Rienzi[4], Filippo M. Ubaldi[4], Alan H. Handyside[1,2,5,7#], and Eva R. Hoffmann[3,#].

[1]The Bridge Centre, London SE1 9RY, UK.

[2]School of Biosciences, University of Kent, Canterbury CT2 7NJ, UK.

[3]MRC Genome Damage and Stability Centre, School of Life Sciences, University of Sussex, Brighton, BN1 9RQ, UK.

[4]G.E.N.E.R.A., Centers for Reproductive Medicine, Rome, Marostica, Umbertide, Italy.

[5]Illumina, Capital Park CPC4, Fulbourn, Cambridge CB21 5XE, UK.

[6]Department of Mathematics and Statistics, University of Indiana, Bloomington, Indiana, US.

[7]Institute of Integrative and Comparative Biology, University of Leeds, Leeds LS2 9JT, UK.

*These authors contributed equally to this work.

[#]Corresponding authors: eh58@sussex.ac.uk, ahandyside@illumina.com

Summary

Defects in segregation lead to missing or lacking chromosomes (aneuploidy) in human eggs, a major cause of pregnancy failure and congenital disorders. Physical exchanges (crossovers) between homologous chromosomes are formed during foetal development and ensure that the pair remains tethered until their separation decades later in the meiotic divisions in adult oocytes. Here, we generate genome-wide maps of crossovers and chromosome segregation patterns by recovering all three products of single female meioses (embryo or oocytes and corresponding polar bodies). Genotyping > 4 million informative single-nucleotide polymorphisms (SNPs) from 23 complete meioses allowed us to map 2,032 maternal and 1,342 paternal crossovers and to infer the segregation patterns from 529 chromosome pairs. We uncover a novel reverse chromosome segregation pattern in which both homologs separate their sister chromatids at meiosis I; detect selection for higher recombination rates in the female germline by the elimination of aneuploid embryos; and report chromosomal drive against non-recombinant chromatids at meiosis II. Collectively, our findings reveal that recombination not only affects homolog segregation at meiosis I but also the fate of sister chromatids at meiosis II.

Main text.

Errors in chromosome segregation during the meiotic divisions in human female meiosis are a major cause of aneuploid conceptions, leading to implantation failure, pregnancy loss, and congenital disorders [1]. The incidence of human trisomies increases exponentially in women from ~ 35 years of age, but despite conservative estimates that 10-30% of natural conceptions are aneuploid[2], the underlying causes and their relative contributions are still unclear. In addition to maternal age, one important factor that is hypothesized to predispose to missegregation in both sexes is altered recombination. Recombinant chromosomes in the offspring are the result of crossovers, the reciprocal exchange of DNA between homologous chromosomes (homologs). Together with sister chromatid cohesion, crossovers physically link the homolog pair together during the prophase stage of meiosis (Fig. 1a), which takes place during foetal development in females. The linkages have to be maintained for decades, because the two rounds of chromosome segregation only occur in the adult woman. By following the pattern of genetic markers such as single nucleotide polymorphisms (SNPs) on the two chromosomes inherited from the mother in trisomic conceptions, it has been inferred that some crossovers occur too close to centromeres[1,3-6], where they may disrupt the cohesion between the two sister chromatids[7,8]. Other crossovers have been suggested to be too far from the centromeres to mediate correct attachment, or to be lacking altogether (non-exchange, E_0)[1,3-6]. If these inferences are correct, it follows that events that shape the recombination landscape in oocytes during foetal development of women affect their risk of having an aneuploid conception decades later in adult life.

A limitation of these extensive population-based studies, however, is that only one of the products of meiosis is analysed (the oocyte). This prevents direct identification of the origin of chromosome segregation errors and provides only partial information on the crossovers during prophase of meiosis I. The ‘missing data’ problem is so significant that

even the meiotic origin of age-related trisomies has been challenged recently[9]. Another confounding factor is that spontaneous miscarriages, still and live births on which our current knowledge is based represent only a minor fraction of the aneuploid embryos at conception. The majority of affected embryos are lost throughout pregnancy resulting in major preclinical and clinical losses[2]. Thus, to understand the origin of human aneuploidies, we need to assess all three meiotic products in unselected oocytes and embryos.

Meiomapping of single meioses in oocytes and embryos.

To follow genome-wide recombination and chromosome segregation simultaneously, we recovered all three products of female meiosis, which include the first and second polar bodies (PB1 and PB2) and the corresponding activated oocytes or fertilised embryos. We refer to these as oocyte-PB or embryo-PB trios (Fig 1a-c). 10 embryo-PB trios were obtained after normal fertilisation of the oocyte following intracytoplasmic sperm injection (ICSI). The embryos reached various stages of preimplantation development and originated from a single donor having preimplantation genetic diagnosis for single gene defect and who consented to follow up genetic analysis of her embryos (Fig. 1a, Extended Data Table 1). A further 13 trios were generated without fertilisation by activating mature MII-arrested oocytes with a calcium ionophore, which induced completion of MII and extrusion of the PB2 (Fig. 1b, Methods). This method was highly successful (85%, n=40, Extended Data Table 2) and did not alter the rate of meiosis II errors in the activated oocytes compared with embryos generated by ICSI (2% versus 1.7%; Table 1). The oocyte-PB trios were obtained from five healthy female donors, who had cryopreserved unfertilised eggs in the course of fertility treatment but having achieved a pregnancy and live birth following IVF, consented to their remaining eggs being activated and undergoing genome analyses. The principle of isolating

all three meiotic products is similar to the approach of using the polar bodies and recovering the female pronucleus from zygotes[10].

The trio datasets were complemented with data on recombination and aneuploidy rates from 29 embryos (without polar bodies) in which SNP genotyping and karyomapping[11] had previously been used for preimplantation genetic diagnosis or screening. Because informative SNPs were available from both the mother and father, we were able to compare recombination in paternal and maternal chromosomes and their association with aneuploidy in embryos (Supplemental Table S1).

All samples were amplified by whole genome amplification and genotyped at approximately 300,000 SNP loci genome-wide[11]. We detected > 4 million informative SNPs at high stringency, which spanned > 92% of the genome, across the 23 complete trios (meioses), with an average resolution of 30 kb. For the oocyte-PB trios, genomic DNA from each donor was also genotyped to identify informative heterozygous SNP loci (hetSNPs). For the oocyte-PB trios, all heterozygous SNPs in the mother's genomic DNA are informative, whereas in embryos, maternal and paternal hetSNPs may be shared. Hence, the pattern of recombination in the paternal chromosomes was analysed by karyomapping (Handyside et al; Natesan et al) and only the two subsets of SNP loci which were heterozygous in the father and homozygous in the mother (or vice versa) were identified and used to phase the two haplotypes from the given parent in the embryo[11,12]. The informative SNPs were phased using 'siblings'[10] that contain only a single chromatid from their mother (PB2, oocytes or maternal chromatid in embryo) or father (embryos). The informative SNPs were phased by selecting a PB2 or oocyte/embryo as a reference (also known as 'assumed ancestor')[10] and inferring the crossover positions in the assumed offsprings (i.e. trios from the same parent; Extended Data Fig. S1). Crossovers in the same position in the assumed offspring are highly unlikely to occur and these common crossovers can therefore be used to re-form the reference genome

from which the two haplotypes can be deduced (Extended Data Fig. S1). Since many of our samples were single cells, we validated our workflow on single cells by comparing recombination maps in 15 individual cells from a donor to the genomic DNA of the child, and by assessing 10 individual blastomeres from the same embryo for direct comparison. In all cases, concordance of recombination frequencies and their positions was > 99%.

A typical MeioMap from a normal embryo-PB trio is shown in Fig 1d. This reveals Mendelian segregation of sequence polymorphisms (green and yellow segregate 2:2 across haplotype regions) and independent assortment of different chromosomes pairs in meiosis I, such that the haploid oocyte contains chromosomes of both yellow and green origin (pericentromeric SNPs are used as a chromosome's fingerprint). Crossovers, which result in recombinant chromosomes, are evident by transitions between the two maternal haplotypes (green or yellow) in the PB2 and oocyte, or between a single maternal haplotype and heterozygous regions (PB1). 39 cases of aneuploidy were detected by the absence or presence of SNPs from an entire chromosome (Table 1). The inferred chromosomal aneuploidies can be observed by array CGH (Extended Data Fig. S2). We also detected three gross structural rearrangements to chromosomes. Since two of the three meiotic products were affected (reciprocal gain and loss), it rules out that these rearrangements occurred during germline development and demonstrates that such rearrangements can occur during meiosis (Extended Data Table 3). Aneuploidy rates and the contribution of MI and MII errors were equally abundant and similar to those expected for this age range (33-41 years; Table 1)[13-17].

All gains and losses were reciprocal and involved two meiotic products, such that a gain in the oocyte was matched by the loss of the chromosome in the PB1 or PB2. Of the 529 chromosome pairs assessed in the trios, we did not detect any deviation from the four chromatids expected to participate in meiosis. These observations firmly establish meiotic errors as the main contributor of aneuploid conceptions and do not support germline

mosaicism in chromosome number prior to meiosis[9] as a significant factor in the maternal age-related increase in human trisomies.

Reverse segregation: a novel chromosome segregation pattern in female meiosis.

To understand the nature of missegregation, we inferred chromosome segregation from the trios by following the informative SNPs at the pericentromere. Trisomies that occur at a high rate in the natural population of women of advanced maternal age[4] were originally hypothesized to arise by MI nondisjunction (MI NDJ) where both homologs segregate to the oocyte at meiosis I, followed by a normal second division[18] (Fig. 2a, Extended Data Fig. S3a). However, cytological examination of human oocytes that failed to fertilise in IVF clinics suggested that precocious separation of sister chromatids (PSSC) was the major cause of human age-related trisomies[19] (Fig. 2a, Extended Data Fig. S3b). Having the genetic identity of the chromatids not only from the embryos or oocytes but also their matched polar bodies allows the two segregation patterns to be distinguished, because the chromosome signatures in the two PBs will differ (Fig. 2a). Confirming previous studies using array CGH for copy number analysis in trios[20], classical meiosis I nondisjunction was relatively rare and precocious separation of sister chromatids was more frequent (Fig. 2a-c). The preponderance of PSSC compared to meiosis I nondisjunction is consistent with findings in oocytes from younger Chinese donors, although aneuploidy rates are much lower in this age group (Fig. 2b)[10].

Unexpectedly, the most frequent non-canonical segregation pattern gave rise to a PB1 that contained two non-sister chromatids (green and yellow fingerprints around the centromere, n=26). In 20 of the 26 instances, both the oocyte and the PB2 contained a normal chromosome content, but with non-sisters instead of sister chromatids (Fig. 2a, Rev Seg). This pattern cannot be detected by copy number analysis used previously[20], since the

complement of chromosomes in the three cells is normal (two chromatids in PB1, and one each in the oocyte and PB2). We refer to this novel pattern as reverse segregation, since we infer that sister chromatids of both homologs separated first in meiosis I, followed by non-sister chromatids (homologs) in meiosis II (Fig. 2d). Both acrocentric and larger metacentric chromosomes displayed this reverse segregation pattern (Fig. 2c), which was observed in oocytes and embryos from all donors, ruling out that it was specific to certain women (Table 2, Extended Data Table S4). In the remaining six cases, the two non-sister chromatids missegregated into the egg or the PB2, resulting in an aneuploid oocyte (Fig. 2a, Rev Seg MII, Extended Data Fig. S3d).

There are several mechanisms that could contribute to the reverse segregation pattern. One intriguing possibility is that the reverse segregation pattern is the result of centromeric crossovers that fall at or within 1-2 Mb of the centromeres, the positions of the last informative SNPs (Supplemental Table S6). Centromeric crossovers interfere with segregation of sister chromatids in *Drosophila*[7] and budding yeast[8], and centromere-proximal crossovers are associated with an increased risk of aneuploidy in human foetuses[1]. Thus, the high incidence of MII nondisjunction (23%, n=26) could be explained by crossover at or within the extreme vicinity of centromeres. Another possible mechanism that seems particularly plausible for the larger metacentric chromosomes where two crossovers would have to occur within 1 Mb on both sides of the centromere, is that homologs segregated their sister chromatids in an equational fashion in MI, followed by a weak preference for accurate non-sister chromatid segregation at MII (77% compared to 50% expected from random; n=26; $p < 0.05$). The equational division at MI is unlikely to be the result of two independent PSSC events, because the observed frequency of both homologs separating their sister chromatids is more than 100× greater than the predicted frequency based on two independent PSSC events ($p < 0.001$). PSSC of one homolog could predispose the second homolog to split its sister

chromatids at anaphase I, or homologs could fall apart during the extended dictyate arrest to generate two univalents. There is some evidence for deterioration of bivalents into two univalents in human MI oocytes[21,22] and this could predispose both univalents to segregate their sister chromatids at meiosis I. Indeed, this is the case in mouse oocytes, where univalents preferentially segregate sister chromatids at meiosis I[23,24]. In either case, at meiosis II, non-sister chromatids could be physically attached or the oocyte may use distributive segregation mechanisms that do not rely on physical attachment between chromosomes. The relative contributions of reverse segregation mechanisms and centromeric crossovers remain to be determined, but in either case demonstrate that events attributed to mistakes in chromosome segregation in meiosis II can have their origin at meiosis I in human female meiosis.

Variation in global recombination rates in oocytes and embryos.

Variation in recombination in foetal oocytes has been hypothesized to give rise to vulnerable crossover configurations that predispose chromosome pairs to missegregation decades later in the adult woman. To assess recombination in adult oocytes and embryos, we mapped 883 maternal crossovers in the oocyte-PB trios and 1149 and 1342 maternal and paternal crossovers, respectively, in the embryos (Fig. 3a; note maternal rates could not be obtained for all embryos). 12% of the reciprocal crossover events occurred between non-sister chromatids in the PB2 and oocyte. A similar proportion would be expected to occur in the PB1 and are undetectable, since the two DNA strands cannot currently be separated and phased individually[10]. Using the 300K SNP arrays gave median resolutions of 107 Kb and 331 Kb for crossovers in the oocyte-PB and embryos, respectively (Fig. 1e). This is similar to high-resolution population-based studies employing SNP arrays[25-27].

Several observations support the conclusion that recombination rates in the adult oocytes and embryos are highly variable, like those seen in unselected, foetal oocytes[28-30]. At the same time, the average recombination frequencies are reminiscent of those reported for human populations. The average number of maternal crossovers in the oocyte or embryos was 41.6 ± 11.3 S.D. (n=51 ; Extended Data Table 4; Supplemental Tables 1-5). This rate is consistent with estimates from foetal oocytes and population-based assessments[10,25,27,31-37] and those in detected in the female pronucleus (42.5 ± 9.0 S.D., n=52)[10]. The frequencies of crossovers detected in the egg correlated well with those in the PB1 or PB2 (Extended Data Fig. S4). The maternal recombination rates and the lengths of haplotype blocks were highly variable between donors as well as within donors[28,29,36,38], varying by as much as two-fold (Fig. 3b, f and g; Extended Data Fig. S4). Using the oocyte-PB trios, maternal crossovers displayed a median distance of 32.4 Mb, which was in excess of the 18.3 Mb predicted by random distribution of crossovers along chromosomes (Methods). This is consistent with crossover interference along homolog pairs[10].

Embryos contain informative markers of both maternal and paternal origin. This allows us to assess recombination of both sexes in unselected embryos for the first time. Maternal recombination rates were 1.63-fold higher than paternal rates in the embryos, consistent with population-based studies and molecular approaches on single sperm and foetal oocytes[20,22,26-32]. The additional maternal recombination events tend to increase recombination on the X chromosome as well as larger chromosomes (Fig. 3d). Maternal recombination was more centromeric compared to paternal events (Fig. 3e, Extended Data Fig. S5), although centromeres tended to suppress nearby recombination[10,20,22,26-32] (Fig. 3f). However, the suppression of centromeric crossovers varied amongst oocyte-PB trios, even within the same woman (Fig. 3g). This variation may predispose some oocytes to crossovers that are too near to centromeres that may interfere with segregation[1]. Collectively, these

observations reveal that the variation in total crossover numbers detected in adult oocytes is analogous to the variation in Mlh1 counts observed in foetal oocytes[28-30], suggesting that Mlh1 foci serve as good proxy for crossover recombination events in human oocytes. Simultaneously, the average recombination rates are reminiscent of those in the human population. This validates our approach and lends support to the hypothesis that the variability in the rates and distribution of recombination events between and within individuals gives rise to vulnerable crossover configurations in foetal oocytes that are propagated to adult oocytes and, ultimately, embryos.

Global recombination rates as a risk factor for aneuploidy.

To understand how the variability of maternal recombination rates affects human aneuploidy, we addressed whether the global, genome-wide recombination rates were correlated with the incidence of aneuploidy in individual oocytes and embryos. Indeed, global recombination rate was a strong predictor of aneuploidy (Fig. 4a), even when we excluded an outlier embryo, which contained 12 aneuploidies and no detectable crossovers amongst any of the chromosome pairs. The recombination rate is an important factor, accounting for 18% of the variation in the incidence of aneuploidy (outlier excluded; permutation test).

If lower global recombination rates predispose oocytes to meiotic chromosome segregation errors, then normal euploid embryos should contain chromosomes that underwent higher maternal genome-wide recombination frequencies than those of aneuploid embryos. To examine whether this was the case, we divided the embryos and oocytes into two groups (euploid or aneuploid) and determined their respective recombination rates (Fig. 4b). Normal, euploid oocytes and embryos had on average, 5.8 recombination events more than aneuploid ones. This difference was significant even when we accounted for crossovers that may not be detected due to the presence of two chromosomes in the aneuploid oocyte[10] (Methods).

Notably, the overlap in the distribution of recombination rates between the euploid and aneuploid groups is consistent with the presence of other factors that influence the fidelity of chromosome segregation[1]. Our findings suggest that higher global recombination frequencies, which are determined during foetal development, protect against errors in chromosome segregation decades later in the adult woman. When errors do occur, they give rise to aneuploidy, many of which are selected against prior to the implantation of the embryo[39]. One implication of this is that recombination rates may be under selection in women as they enter their 30s, increasing rates by as much as 14% in women of advanced maternal age (5.8/41.5, the overall average). Elimination of aneuploid embryos that contain lower recombination rates could contribute towards the higher female-specific recombination rate observed in the human population. Since crossover frequencies are determined by the rate of initiation of double-strand breaks and the outcome of repair (crossover or noncrossover), mechanisms that alter either could be selected for in female meiosis. Notably, alleles that contribute to female-specific recombination rates have been identified in genome-wide association studies[35-38]and it has long been appreciated that chromosome structure is altered in female meiosis, with chromosomes having a longer axis and shorter chromatin loops[40]. The increased loop number correlates with the increased recombination rate in female meiosis[30,40].

Non-recombinant chromatids are at risk of precocious sister chromatid separation at meiosis I.

How do global recombination rates affect the segregation outcomes of individual homolog pairs? We hypothesized that lower global recombination rates might increase the risk of generating vulnerable crossover configurations. We first considered non-exchange E_0 homolog pairs, which would give rise to trios, where the PB1 contains one homolog (green or

yellow) and the oocyte and PB2 one sister each from the other homolog (Extended Data Fig. S6a). Of 529 chromosome pairs, no such example was observed in our data, although one case was observed by Hou *et al*. (Hou, pers. comm.). E_0 may be extremely rare, or another possibility is that they missegregate. Indeed, we observed 13 presumed E_0 from the 529 chromosome pairs across the 23 trios (Extended Data Fig. S6a-d). The overall incidence (2.6%, n= 506) and the overrepresentation of the two smallest chromosomes (21 and 22) are reminiscent of observations of cytological markers for crossovers on foetal chromosomes in meiotic prophase[28-30]. The observed incidence of presumed E_0 was much lower than expected if crossovers were randomly distributed amongst chromosomes (Extended Data Fig. S6h), suggestive of crossover assurance mechanism(s) in human oocytes. None of the presumed E_0 chromosomes followed a classical meiotic segregation pattern. Instead they all underwent PSSC or reverse segregation (with or without MII missegregation; Extended Data Fig. S6). The latter is consistent with the bi-orientation of univalent chromosomes at meiosis I in model organisms[23,24].

Informative SNPs on missegregated chromosomes cannot be phased, making crossovers undetectable (Extended Data Fig. S6). However, from the polar body analysis most of the presumed E_0 contained non-recombinant chromatids (R_0). Fig. 4c shows that global recombination rates are important for determining the generation of R_0, which in turn are at increased risk of missegregation compared to fully recombinant bivalents (all four chromatids engaged in recombination; “rec”, Fig. 4d). Bivalents that contained a R_0 were preferentially involved in PSSC, suggesting that non-recombinant chromatids are at risk of precociously separating from their sister at meiosis I. It is possible that non-recombinant chromatids are at elevated risk of becoming dissociated from the rest of the bivalent during the decades-long dictyate arrest[41,42]. We conclude that recombination affects not only the

generation and segregation of putative non-exchange homolog pairs, but also influences the dynamics of sister chromatid segregation.

Meiotic drive for recombinant chromatids at meiosis II.

Recombination does not only affect segregation of sister chromatids at meiosis I, but also at meiosis II. The MeioMaps revealed 135 chromatids in the oocyte or PB2 that were non-recombinant and had segregated normally (Fig. 5a). These R_0 are expected to be randomly distributed amongst the oocyte and the PB2. Contrary to this expectation, R_0 were nearly twice as likely to be found in the PB2 than the oocyte. The selection appears to be against non-recombinant chromatids, because when both sisters recombined, their segregation was random and the recombination rates were similar in the oocyte and PB2 (Extended Data Table 4). We infer that when the two sister chromatids segregated at meiosis II, non-recombinant chromatids were preferentially driven into the PB2 and thus eliminated from the human germline (Fig. 5b,c). The use of the asymmetric cell divisions during oogenesis for the preferential inclusion of an allele[43] or even whole chromosomes[44-46] is referred to as meiotic or chromosomal drive. The meiotic drive against non-recombinant chromatids resulted in a 6.6% elevation in the recombination rates in oocytes compared to the PB2s (Extended Data Table 4). These findings imply that recombination is not only important for the accurate segregation of homologs at meiosis I, but also acts as a driving force during sister chromatid segregation at meiosis II. Selection against non-recombinant chromatids may prevent entire chromosomes from being inherited as a single haplotype block, thereby reducing the probability of inbreeding or propagation of segregation distorters[47-49]. This may be significant in terms of population structure and the genomic health of children. The difference in genome structure between the PB2 and oocyte is particularly relevant, because the PB2 has been proposed for use in treatment of mitochondrial disease[50].

DISCUSSION.

Until recently, recombination was studied in populations, where missing polar body information was not available; or in foetal oocytes, which arise decades prior to the segregation events being studied. MeioMaps from unselected adult oocytes, the female pronucleus in zygotes[10], and embryos, now provide a 'missing link' between events that occur during foetal development and their influence on chromosome segregation outcomes decades later in the adult oocyte. MeioMaps provide compelling evidence that the high degree of variation in recombination rates between and within women is conserved from foetal to adult oocytes[28-30] and in conceptions[10] (Fig. 3). This implies that the oocytes remain relatively unselected in terms of recombination rates throughout development, which includes the severe phases of atresia during which > 96% of foetal oocytes are culled prior to adulthood. Our findings show that it is this broad variation that leads to lower recombination rates in some eggs, which in turn predispose to them to aneuploidy decades later. Lower genome-wide recombination rates increase the risk of generation of at least two types of vulnerable crossover configurations: non-recombinant chromatids (R_0) and putative non-exchange homologs (E_0). It follows that mechanisms that regulate the distribution of crossovers amongst chromosome pairs (crossover assurance) and between sister chromatids potentiate the risk that lower recombination rates exert on the generation of such vulnerable crossover configurations.

We found recombination rates explained a significant portion of the variation in aneuploidy (18%), whereas another study of younger donors found a weaker contribution[10]. How age and recombination interact to influence segregation of chromosomes, including reverse segregation and meiotic drive against non-recombinant chromatids, is currently unclear as oocytes from younger donors did not show these features[10]. Findings from several

population studies are consistent with the interpretation that higher genome-wide recombination rates are important for chromosome segregation and fertility[26,33,35,51] and become increasingly important as women age[25,33]. Our observations suggest that higher recombination rates protect the oocyte against aneuploidy in women of advanced maternal age, which are therefore more likely to give rise to an euploid conception and live birth. Several genome-wide association studies have identified variant SNPs that affect maternal recombination rate [33,35,38,51]. It is conceivable these could be used as biomarkers to stratify risk of age-related aneuploidy in women.

METHODS SUMMARY.

Ethics statement.

All material for the study was ethically sourced with fully informed patient consent. All oocytes for the study were obtained from donors after completion of their IVF treatment and were destroyed for analysis. The oocytes used were vitrified in accordance with Italian law in place at the time of oocyte retrieval for IVF treatment. Use of the oocytes for the study was approved by the Institutional Review Board of the Valle Giulia Clinic where the oocytes were stored and did not influence patient treatment. All embryo samples for the study were either obtained by tubing embryos in their entirety (destroyed) for analysis following a previous abnormal outcome in clinical tests or reanalysis of a clinical biopsy samples after embryos were transferred, stored or discarded depending on the clinical result. SNP genotyping was performed as clinical follow up/validation of clinical genetic analysis and covered by the HFEA. All primary data were encoded such that informative SNPs were represented as A and B. Only secondary data with informative SNPs encoded A and B were used for data analysis. All other methods are covered in the Supplemental Methods section.

ACKNOWLEDGEMENTS.

We are thankful to Celia May, Adam Eyre-Walker, Jennifer Gruhn, Ross Rowsey, James Turner, Francesca Cole, and members of the Hoffmann lab for discussion and critical reading of the manuscript. We thank Yu Hou, Wei Fan, and Sunney Xie for freely sharing data and discussion on their study of female pronucleus-PB trios. Financial support for this research was provided by the MRC (Senior Research Fellowship to ERH; G0902043) and an EMBO Young Investigator award to ERH.

AUTHOR CONTRIBUTIONS.

AC, CO, DC, LR, FU, KS, MS, and AT were responsible for donor consenting, oocyte collection and oocyte activation. LR, FU, AH, KS oversaw ethical and legal regulation in Italy and the UK. AC, CO, SN, HJ, DC carried out amplification, SNP array and array CGH experiments. AH, LJN, CO, ERH analysed the encoded data. ERH and ADH carried out data analysis and simulations; ERH and EH carried out statistical analyses; ERH, AH and LJN generated the figures; ERH, AH, LJN, CO wrote the manuscript; AH, CO, AC, LN and ERH, edited the manuscript. All authors proof-read and accepted the manuscript.

AUTHOR INFORMATION.

The authors declare no competing financial interest.

Correspondence and requests for data should be addressed to ERH (eh58@sussex.ac.uk) or AH (ahandyside@illumina.com).

References.

1 Nagaoka, S. I., Hassold, T. J. & Hunt, P. A. Human aneuploidy: mechanisms and new insights into an age-old problem. *Nat Rev Genet* **13**, 493-504 (2012).

2 Hassold, T. & Hunt, P. To err (meiotically) is human: the genesis of human aneuploidy. *Nat Rev Genet* **2**, 280-291 (2001).

3 Zaragoza, M. V. *et al.* Nondisjunction of human acrocentric chromosomes: studies of 432 trisomic fetuses and liveborns. *Hum Genet* **94**, 411-417 (1994).

4 Hassold, T. J. & Jacobs, P. A. Trisomy in man. *Annu Rev Genet* **18**, 69-97 (1984).

5 Hassold, T. *et al.* A cytogenetic study of 1000 spontaneous abortions. *Ann Hum Genet* **44**, 151-178 (1980).

6 Freeman, S. B. *et al.* The National Down Syndrome Project: design and implementation. *Public Health Rep* **122**, 62-72 (2007).

7 Koehler, K. E. *et al.* Spontaneous X chromosome MI and MII nondisjunction events in *Drosophila melanogaster* oocytes have different recombinational histories. *Nat Genet* **14**, 406-414 (1996).

8 Rockmill, B., Voelkel-Meiman, K. & Roeder, G. S. Centromere-proximal crossovers are associated with precocious separation of sister chromatids during meiosis in *Saccharomyces cerevisiae*. *Genetics* **174**, 1745-1754 (2006).

9 Hulten, M. A., Patel, S., Jonasson, J. & Iwarsson, E. On the origin of the maternal age effect in trisomy 21 Down syndrome: the Oocyte Mosaicism Selection model. *Reproduction* **139**, 1-9 (2010).

10 Hou, Y. *et al.* Genome analyses of single human oocytes. *Cell* **155**, 1492-1506 (2013).

11 Handyside, A. H. *et al.* Karyomapping: a universal method for genome wide analysis of genetic disease based on mapping crossovers between parental haplotypes. *J Med Genet* **47**, 651-658 (2010).

12 Natesan, S. A. *et al.* Genome-wide karyomapping accurately identifies the inheritance of single-gene defects in human preimplantation embryos in vitro. *Genet Med* **16**, 838-45 (2014).

13 Alfarawati, S. *et al.* The relationship between blastocyst morphology, chromosomal abnormality, and embryo gender. *Fertil Steril* **95**, 520-524 (2011).

14 Kuliev, A., Zlatopolsky, Z., Kirillova, I., Spivakova, J. & Cieslak Janzen, J. Meiosis errors in over 20,000 oocytes studied in the practice of preimplantation aneuploidy testing. *Reprod Biomed Online* **22**, 2-8 (2011).

15 Gutierrez-Mateo, C. *et al.* Validation of microarray comparative genomic hybridization for comprehensive chromosome analysis of embryos. *Fertil Steril* **95**, 953-958 (2011).

16 Capalbo, A. *et al.* Sequential comprehensive chromosome analysis on polar bodies, blastomeres and trophoblast: insights into female meiotic errors and chromosomal segregation in the preimplantation window of embryo development. *Hum Reprod* **28**, 509-518 (2013).

17 Franasiak, J. M. *et al.* The nature of aneuploidy with increasing age of the female partner: a review of 15,169 consecutive trophectoderm biopsies evaluated with comprehensive chromosomal screening. *Fertil Steril* **101**, 656-663 (2014).

18 Reiger, R., Michaelis, A. & M.M., G. *Glossary of genetics and cytogenetics*. (Springer Verlag, Berlin, Heidelberg, New York, 1968).

19 Angell, R. R. Predivision in human oocytes at meiosis I: a mechanism for trisomy formation in man. *Hum Genet* **86**, 383-387 (1991).

20 Handyside, A. H. *et al.* Multiple meiotic errors caused by predivision of chromatids in women of advanced maternal age undergoing *in vitro* fertilisation. *Eur J Hum Genet* **20**, 742-747 (2012).

21 Angell, R. First-meiotic-division nondisjunction in human oocytes. *Am J Hum Genet* **61**, 23-32 (1997).

22 Garcia-Cruz, R. *et al.* Cytogenetic analyses of human oocytes provide new data on non-disjunction mechanisms and the origin of trisomy 16. *Hum Reprod* **25**, 179-191 (2010).

23 LeMaire-Adkins, R. & Hunt, P. A. Nonrandom segregation of the mouse univalent X chromosome: evidence of spindle-mediated meiotic drive. *Genetics* **156**, 775-783 (2000).

24 Kouznetsova, A., Lister, L., Nordenskjold, M., Herbert, M. & Hoog, C. Bi-orientation of achiasmatic chromosomes in meiosis I oocytes contributes to aneuploidy in mice. *Nat Genet* **39**, 966-8 (2007).

25 Coop, G., Wen, X., Ober, C., Pritchard, J. K. & Przeworski, M. High-resolution mapping of crossovers reveals extensive variation in fine-scale recombination patterns among humans. *Science* **319**, 1395-1398 (2008).

26 Middlebrooks, C. D. *et al.* Evidence for dysregulation of genome-wide recombination in oocytes with nondisjoined chromosomes 21. *Hum Mol Genet*, 408-417 (2013).

27 Kong, A. *et al.* A high-resolution recombination map of the human genome. *Nat Genet* **31**, 241-247 (2002).

28 Lenzi, M. L. *et al.* Extreme heterogeneity in the molecular events leading to the establishment of chiasmata during meiosis i in human oocytes. *Am J Hum Genet* **76**, 112-127 (2005).

29 Cheng, E. Y. *et al.* Meiotic recombination in human oocytes. *PLoS Genet* **5**, e1000661 (2009).

30 Gruhn, J. R., Rubio, C., Broman, K. W., Hunt, P. A. & Hassold, T. Cytological studies of human meiosis: sex-specific differences in recombination originate at, or prior to, establishment of double-strand breaks. *PLoS One* **8**, e85075 (2013).

31 Broman, K. W., Murray, J. C., Sheffield, V. C., White, R. L. & Weber, J. L. Comprehensive human genetic maps: individual and sex-specific variation in recombination. *Am J Hum Genet* **63**, 861-869 (1998).

32 Tease, C., Hartshorne, G. M. & Hulten, M. A. Patterns of meiotic recombination in human fetal oocytes. *Am J Hum Genet* **70**, 1469-1479 (2002).

33 Kong, A. *et al.* Recombination rate and reproductive success in humans. *Nat Genet* **36**, 1203-1206 (2004).

34 Myers, S., Bottolo, L., Freeman, C., McVean, G. & Donnelly, P. A fine-scale map of recombination rates and hotspots across the human genome. *Science* **310**, 321-324 (2005).

35 Kong, A. *et al.* Sequence variants in the *RNF212* gene associate with genome-wide recombination rate. *Science* **319**, 1398-1401 (2008).

36 Kong, A. *et al.* Fine-scale recombination rate differences between sexes, populations and individuals. *Nature* **467**, 1099-1103 (2010).

37 Kong, A. *et al.* Common and low-frequency variants associated with genome-wide recombination rate. *Nat Genet* **46**, 11-16 (2014).

38 Chowdhury, R., Bois, P. R., Feingold, E., Sherman, S. L. & Cheung, V. G. Genetic analysis of variation in human meiotic recombination. *PLoS Genet* **5**, e1000648 (2009).

39 Capalbo, A. *et al.* Correlation between standard blastocyst morphology, euploidy and implantation: an observational study in two centers involving 956 screened blastocysts. *Hum Reprod* **29**, 1173-1181 (2014).

40 Lynn, A. *et al.* Covariation of synaptonemal complex length and mammalian meiotic exchange rates. *Science* **296**, 2222-2225 (2002).

41 Wolstenholme, J. & Angell, R. R. Maternal age and trisomy--a unifying mechanism of formation. *Chromosoma* **109**, 435-438 (2000).

42 Garcia-Cruz, R. *et al.* Dynamics of cohesin proteins REC8, STAG3, SMC1 beta and SMC3 are consistent with a role in sister chromatid cohesion during meiosis in human oocytes. *Hum Reprod* **25**, 2316-2327 (2010).

43 Sandler, L. & Novitski, E. Meiotic Drive as an Evolutionary Force. *Am Nat* **91**, 105-110 (1957).

44 Bongiorni, S., Fiorenzo, P., Pippoletti, D. & Prantera, G. Inverted meiosis and meiotic drive in mealybugs. *Chromosoma* **112**, 331-341 (2004).

45 Pardo-Manuel de Villena, F. & Sapienza, C. Nonrandom segregation during meiosis: the unfairness of females. *Mamm Genome* **12**, 331-339 (2001).

46 Dawe, R. K. & Cande, W. Z. Induction of centromeric activity in maize by suppressor of meiotic drive 1. *Proc Natl Acad Sci U S A* **93**, 8512-8517 (1996).

47 Haig, D. & Grafen, A. Genetic scrambling as a defence against meiotic drive. *J Theor Biol* **153**, 531-558 (1991).

48 Chmatal, L. *et al.* Centromere strength provides the cell biological basis for meiotic drive and karyotype evolution in mice. *Curr Biol* **24**, 2295-2300 (2014).

49 Brandvain, Y. & Coop, G. Scrambling eggs: meiotic drive and the evolution of female recombination rates. *Genetics* **190**, 709-723 (2012).

50 Wang, T. *et al.* Polar body genome transfer for preventing the transmission of inherited mitochondrial diseases. *Cell* **157**, 1591-1604 (2014).

51 Stefansson, H. *et al.* A common inversion under selection in Europeans. *Nat Genet* **37**, 129-137 (2005).

52 Kuwayama, M. Highly efficient vitrification for cryopreservation of human oocytes and embryos: the Cryotop method. *Theriogenology* **67**, 73-80 (2007).

53 Kuwayama, M., Vajta, G., Kato, O. & Leibo, S. P. Highly efficient vitrification method for cryopreservation of human oocytes. *Reprod Biomed Online* **11**, 300-308 (2005).

54 Wickham, H. ggplot2: Elegant Graphics for Data Analysis. *Use R*, 1-212 (2009).

Table 1. Origin and incidence of maternal aneuploidies.

Dataset:	Mean maternal age[a]	n[b]	% aneuploid oocytes	Chromosome missegregation events[d]							Total chr
				All events	Aneuploid outcome in oocyte	Gain in oocyte		Loss in oocyte			
						MI	MII	MI	MII		
Oocyte-PB trios	37.3 (33-41)	13	62%	26	12	2	4	4	2		299
Embryo-PB trios	38.3	10	70%	19	8	4	1	0	3		230
Embryo only	37.1 (34-42)	29[c]	54%	n.d.	19	5	4	n.d	n.d.		667

[a] Mean age and range.

[b] Number of trios or embryos analysed

[c]28 embryos and 1 chorionic villus sample.

[d]Statistical test for significance of MII nondisjunction rates in oocyte-PB and embryo-PB trios: 6 out of 299 compared to 4 out of 230, respectively, G-test with Williams' correction, $p = 0.82$.

n.d., not determined since no information from polar bodies.

Table 2. Incidence of reverse segregation

Sample type	Incidence	Chromosomes involved
Oocyte-PB1 duos (unactivated)[a]	8.7 ± 4.2% (n=46)	4, 13, 14, 16
Oocyte-PB1-PB2 trios	3.7 ± 1.1% (n=299)	4, 11, 14, 15, 16, 19, 22
Embryo-PB1-PB2 trios	7.2 ± 1.8% (n=207)	4, 9, 16, 17, 19, 21, 22

[a] See Fig. 2e. Reverse segregation was observed in all donors (Extended Data Table S4).

Figure legends.

Figure 1. Human MeioMaps from embryos and oocytes together with their corresponding polar bodies. Combined recombination and chromosome segregation patterns were inferred by retrieving and SNP typing all three meiotic products from single meioses.

(a,b) The two maternal chromosomes and their genotypes are shown in green and yellow, respectively. Crossovers in the primary oocyte occurs during foetal development and are shown in the dashed box. The two polar bodies were sequentially biopsied to avoid misidentification (shown by grey vertical arrows). Maternal MeioMaps were deduced from the embryo following intracytoplasmic sperm injection **(ICSI)** or directly assessed in the haploid oocyte, after artificial activation *(b)*.

(c) Example of an activated oocyte with a single pronucleus (arrow) and extruded PB2.

(d) An example of a MeioMap from a normal meiosis after individual processing of the three cells following MDA amplification, genome-wide SNP detection, and phasing (see Methods). Each chromosome is represented by three vertical columns of the three cells of the trio (PB1, PB2, and embryo or oocyte). The two maternal phased haplotypes are represented by green and yellow. Blue represents the detection of both haplotypes. Regions where SNPs are not available on the array are shown in white (repetitive sequences on chr. 1 and 9) or gray (rDNA). Black bars illustrate the position of the centromere. Red bars shows the last informative SNPs to call. Crossovers are manifested as reciprocal breakpoints in haplotypes (green to yellow, blue to green, etc.) in two of the three cells. Note that the colours of the haplotype blocks between different chromosomes are not necessarily derived from the same grandparent. Histograms of the resolution of the crossovers are shown in

(***e***). The resolution was 352 Kb and 311 Kb for maternal (m) and paternal (p) crossovers in the embryos, respectively.

Figure 2. MeioMaps reveal origin of aneuploidies and a novel chromosome segregation pattern.

(***a***) Segregation patterns revealed from following the pericentromeric haplotypes (yellow and green around centromere) in all three products of female meiosis. Only examples leading to trisomic conceptions are shown. For all possible segregation patterns detected by Meiomapping see Extended Data Figure S3. MI NDJ: meiosis I nondisjunction; Rev Seg reverse segregation; PSSC: precocious separation of sister chromatids; MII NDJ: meiosis II nondisjunction.

(***b***) Incidence and type of segregation errors in oocyte-PB and embryo-PB trios. Errors detected in MeioMaps generated from the female pronucleus (FPN-PB) from a younger donor population[10] are shown for comparison The number of donors and average (av.) age are shown. Age ranges were 25-35for FPN-PB[10] and 33-41 for oocyte-PB trios (Extended Data Table 2). The embryo donor was 38 years of age (Extended Data Table 1).

(***c)*** Chromosome abnormalities that resulted in aneuploid oocytes or embryos (upper panel) and all non-canonical segregation patterns (lower panel).

(***d,e***) Inferred mode of reverse segregation (Rev Seg) and detection of the unactivated intermediate (oocyte-PB1 duo, *e*) . Frequencies are shown in Table 2. Alternative segregation outcomes at meiosis II (euploid and aneuploid, n=26; $p < 0.025$; binomial exact test with correction for continuity).

Figure 3. Variation in genome-wide recombination rates between and within individuals.

(a) Boxplot of global recombination rates for oocyte-PB trios, oocytes only, embryo-PB trios and embryos only (maternal and paternal). Note that maternal recombination rates are 1.6-fold higher than paternal rates. On the right, the boxplot shows global recombination rates for

foetal oocytes at the pachytene stage as measured by Mlh1 foci[30] (Gruhn) and for female pronucleus-PB trios from adult Chinese donors[10] (Hou).

(b) Global recombination rates for the 10 donors used in this study. Black circles denote maternal recombination rates for oocyte or embryo only whereas magenta circles show maternal recombination rates for complete oocyte-PB (donors: G04, G06, G07, G08, G09) and embryo-PB trios (LB03).

(c) Distribution of distances between crossovers (Mb).The simulated median distance based on random distribution is 18.3 Mb (Methods). The fitted curve is based on maximum likelihood estimation of a gamma distribution, with shape 2.6141 ± 0.14 (S.E.) and rate 0.066 ± 0.0039 (S.E.). The estimated mean for this fit is 39.3 Mb. Log-likehood of fitting: -2802.738 ; AIC: 5609.476. Centromeric distances were not included from the inter-crossover distances that spanned centromeres. ***(d)*** Average maternal and paternal recombination events on a chromosome-specific basis (embryos; Supplemental Table S1). Error bars denote the standard deviation. GLM analysis revealed that chromosome size had a significant effect on sex-specific recombination frequencies. Spearman correlation test is shown for the p-value for individual, pair-wise comparisons between maternal and paternal recombination frequencies per chromosome. As chromosome size decreases, the contribution of sex to crossover frequencies decreases (Supplemental Raw Data, Fig. 3d).

(e) Crossover position relative to centromeres (CEN), normalized to chromosome length. Statistics: Two-sided Kolmogorov-Smirnov test of normalized length (shown) and absolute length; $p < 0.0005$) after removing the X chromosome. Absolute lengths are shown in Extended Data Fig. S5.

(f) Length of haplotype blocks (not inter-crossover distances), classified according to location relative to telomeres (blue), spanning centromeres (light red), or interstitial (green). Statistics: non-parametric ANOVA for ‘type’ (telomeric, centromeric or interstitial; $p < 0.0001$). The

distances that included a centromere were not adjusted to include the ~ 3×10^6 base pairs of alpha-satellite DNA.

(***g***) Variation in centromere repression of crossovers in oocyte-PB trios from the same donor.

Figure 4. Higher global recombination rates protect against aneuploidy and are selected for in the human female germline.

(***a***) Logistic regression of the frequency of aneuploid chromosomes as a function of global recombination rate in the embryo or oocyte. Black lines shows logistic regression model and 95% confidence interval (dashed line; binomial family). When the outlier with 0 recombination events was omitted, the regression coefficient β was -0.06 and still highly significant ($p < 0.003$). The outlier was omitted from all subsequent statistical analyses.

(***b***) Recombination rates in normal versus aneuploid oocytes and embryos. The arithmetic mean is shown above of the median (magenta, vertical bar). Statistics: Mann-Whitney-Wilcoxon test; one-sided.

(***c***) Incidence of bivalents containing at least one non-recombinant chromatid (R_0) as a function of global recombination rates in oocyte-PB and embryo-PB trios. Statistics as in (*a*).

(***d***) Segregation errors amongst chromosomes that contained one or more R_0 or where all four chromatids had recombined ('rec') . p-values from G-test of heterogeneity (two-sided) are shown.

Figure 5. Meiotic drive for recombinant chromatids at meiosis II increases recombination rates in the human female germline.

(***a***) Sister chromatids are expected to segregate randomly at meiosis II. However, when chromosomes that contained one non-recombinant chromatid and one recombinant one

segregated, the recombinant chromatids was twice as likely to segregate to the oocyte. G-test for proportions (two-sided).

(***b***) Number of R_0 chromosomes segregating to PB2 or oocyte

(***c***) Diagrammatic representation of meiotic drive for recombinant chromatids at meiosis II in the human female germline.

Extended Data Figure Legends

Extended Data Fig. S1. Phasing of maternal haplotypes. Maternal informative SNPs are phased using the 'assumed ancestor' method[10]. A haploid cell containing a single chromatid (1C; either PB2 or Egg) is chosen as the 'assumed ancestor' or reference. Trios from the same mother (or father) are 'assumed offspring'. Using the reference, crossovers in all other assumed offspring are mapped where haplotypes changes compared to the assumed ancestral phasing. Crossovers shared between sibling trios (or assumed offspring; red boxes) can be used to infer crossovers in the assumed ancestor. Iterative phasing using all available oocytes and PB2 allows deduction of the maternal haplotypes.

Extended Data Fig. S2. Validation of whole chromosome aneuploidy by array CGH. An example of chromosome segregation abnormalities inferred from the SNP array patterns in oocyte-PB trios and confirmed by array CGH of the same amplified DNA from all three samples. The green and pink lines are the internal female sample and the blue trace indicates the male reference. The $\log_2$ ratio of the X chromosomes of the reference genomes are used as internal calibration of whole chromosome loss or gain. The MeioMaps for three chromosomes in the same oocyte-PB trio are shown below the aCGH traces (G04_1). For

chromosome 13, three chromatids segregated to the first polar body, a single chromatid was present in the second polar body and none in the oocyte. This is consistent with precocious separation of sister chromatids (PSSC) at meiosis I. Chromosome 20 segregated normally at meiosis I (normal PB1), but there was a gain in the oocyte and corresponding loss in PB2, consistent with a meiosis II nondisjunction. Chromosome 22 underwent a partial gain in PB1 and corresponding loss in the oocyte. This is consistent with a gross structural rearrangement whereby the majority of chromosome 22 segregated to the PB1 along with the intact homolog (Extended Data Table S3). In the SNP representations, yellow and green blocks represent the two different grandparental haplotypes and blue regions denote regions where both haplotypes are present. All aneuploidies in the oocyte-PB trio dataset were verified using array CGH. Validation for embryos has been published previously[12].

Extended Data Fig. S3. Non-canonical segregation patterns-.

(***a***) Meiosis I nondisjunction yields a PB1 containing all four chromatids and empty oocyte and PB2 (upper panel); or an empty first polar body and two non-sister chromatids in the oocyte and PB2 (lower panel).

(***b***) Precocious separation of sister chromatids (PSSC) has four possible segregation outcomes (*i* – *iv*). The green homolog has separated precociously at meiosis I and the yellow homolog segregates normally either to the oocyte (top panel) or the PB1 (lower panel). At meiosis II, the green chromatid segregates randomly to the oocyte (i) and (iii), or to the PB2, (ii) and (iv). Note that one of the nine PSSC involved a structural change in combination with the precocious separation of the sister chromatids in meiosis I.

(***c***) Meiosis II nondisjunction results in two sister chromatids in either the oocyte or PB2 (shown for green only). This pattern could also arise from an earlier PSSC event, where the two sister chromatids have come apart and both stay in the oocyte at meiosis I.

(d) Reverse segregation. Both homologs segregate their sister chromatids at MI, giving rise to an intermediate where both the oocyte and PB1 contains the correct content, but two different sister chromatids (Figure 2e). At meiosis II, the two non-sister chromatids either segregate into the PB2 and oocyte; remain in the oocyte, or both segregate to the PB2 (Fig. 2d). Dotted boxes highlight three different segregation errors that would give rise to the same pattern of maternal pericentromeric SNPs in a trisomic conception (i.e. two non-sister chromatids). Without the information from the polar bodies, these three patterns are indistinguishable.

Extended Data Fig. S4. Correlation of recombination detected in the oocytes and polar bodies.

(a-c) Spearman correlation (ρ) between crossover frequencies per meiosis estimated from the oocyte-PB trio and correlated with counts in PB1 only ***(a)***, oocyte only ***(b)***, and PB2 ***(c)***.

(d) Correlation of crossover events detected in the oocyte compared to the PB2. (n= 13; 5 donors).

(e) Heterogeneity in haplotype lengths in the five different oocyte-PB donors.

Extended Data Fig. S5. Chromosome-specific responses to recombination rates and positions in male and female meiosis.

(a) Density curves of the normalized distance of crossovers to centromeres (CEN). Statistics: Kolmogorov-Smirnov test, two-sided.

(b,c) Histograms and density curves of absolute distances of crossovers to centromeres. Statistics: Kolmogorov-Smirnov test, two-sided.

(d) Chromosome-specific responses in crossover position along chromosomes in the two sexes.

Extended Data Fig. S6. Crossover assurance in human female meiosis.

(a) A non-exchange or exchange-less chromosome pair (E_0) (left). In normal meiosis, non-exchange chromosome pairs can be detected by a single haplotype in the PB1 and the other haplotype in the oocyte and PB2.

(*b*) E_0 that undergo reverse segregation *(b)* cannot be detected directly. This is because the informative SNPs on the two chromatids in the PB1 cannot be phased, hence potential crossovers (far right) cannot be detected.

(*c*) PSSC can result in three chromatids in the PB1. Both maternal SNPs will be present along the entire chromosome (blue). Reciprocal crossovers cannot be mapped, hence the lack of crossovers can only be presumed.

(d-g) Trios with chromosomal content consistent with presumed exchange-less (E_0) homologs due to reverse segregation (RS) resulting in two aneuploid cells *(d)*, reverse segregation resulting in normal chromosomal content in all three cells *(e)*, precocious separation of sister chromatids (PSSC) with an aneuploid *(f)* or euploid oocyte *(g)*.

(h) Modelled risk of a chromosome pair failing to receive a crossover (E_0) as a function of global recombination rates, using the range of rates observed in our datasets. Crossovers were allocated randomly to chromosomes with weighted probability using the chromosome length, thus longer chromosomes receive more crossovers. Data are from 10,000 simulations (see Extended Methods).

EXTENDED DATA TABLES

File name: Extended Data Tables

Extended Data Table 1. Donor information of embryos.

Extended Data Table 2. Donor information of oocyte-PB trios.

Extended Data Table 3. Structural rearrangements to chromosomes in meiosis.

Extended Data Table 4. Summary of recombination and chromosome segregation in all trios.

RAW DATA & SUPPLEMENTAL DATA

Raw data for Figures where required. Data for subpanels are included in separate worksheets, within the EXCEL file:

Fig1_RawData.xlsx

Fig2_RawData.xlsx

Fig3_RawData.xlsx

Fig4_RawData.xlsx

Fig5_RawData.xslx

Fig_S4_RawData.xlsx (Extended Data Fig. S4)

Fig_S5_RawData.xlsx (Extended Data Fig. S5)

Fig_S6_RawData.xlsx (Extended Data Fig. S6).

SUPPLEMENTAL DATA TABLES:

Ottolini_SupplementalTables.xlsx

Contains:

Supplemental Table 1 : Recombination frequencies in embryos

Supplemental Table 2 : Map distances in embryos

Supplemental Table 3 : Crossovers in oocytes

Supplemental Table 4 : Recombination frequencies in oocytes

Supplemental Table 5: Map distances in oocytes

Supplemental Table 6: hetSNP or informative SNP resolution near centromeres of chromosomes undergoing reverse segregation.

METHODS.

METHODS.

Oocyte-PB trios

Patient participation and consent

All MII oocytes for the study were obtained from patients undergoing ICSI treatment in the Centre for Reproductive Medicine GENERA in Rome between 2 September 2008 and 15 May 2009 following controlled ovarian hyperstimulation performed using two different protocols: GnRH-agonist long protocol and GnRH-antagonist protocol. According to the Italian law in force when these oocytes were collected, a maximum of three oocytes could be inseminated per patient. The remaining MII oocytes were vitrified and later recruited for the study after informed consent was obtained from the patients. The study and the informed consent were approved by the Institutional Review Board of the Valle Giulia Clinic and did not influence patient treatment.

Oocyte collection

Oocyte collection was performed at 35 h post-hCG administration. Removal of the cumulus mass was performed by brief exposure to 40 IU/ml hyaluronidase solution in Sage fertilization medium + 10% human serum albumin (HSA) (Cooper Surgical, USA), followed by mechanical removal of the corona radiata with the use of plastic "denuding" pipettes of defined diameters (COOK Medical, Ireland) in a controlled 6% CO_2 and 37°C environment. This procedure was performed between 37 and 40 h post-hCG administration. MII oocytes were then identified for vitrification.

Oocyte vitrification and warming

The vitrification and warming procedures were performed according to Kuwayama *et al*. [52,53]. Commercially available vitrification and warming kits were used (Kitazato BioPharma Co.,

Japan). The vitrification procedure was performed a maximum of 40 hours post hCG administration. The oocytes were stored on a cryotop vitrification tool (Kitazato BioPharma Co., Japan) with a plastic cap for protection during storage in liquid nitrogen. All oocytes were stored submerged in liquid nitrogen until warming was performed. Following oocyte warming degenerated oocytes were discarded and the surviving oocytes were cultured before biopsy of the first polar body (PB1) and activation.

Oocyte culture and activation

All oocyte culture was performed at 37°C in 6% CO_2 and 5% O_2. To enable tracking of the oocytes and PBs, individual culture was performed and culture drops and wells were numbered to allow traceability throughout the experiment.

Immediately after warming, the surviving oocytes were allocated to individually numbered 35 µl microdrops of Sage cleavage medium + 10% HAS under mineral oil (Cooper Surgical, USA) and cultured for 2 hours prior to PB1 biopsy and activation.

Oocytes were activated by exposure to activation medium: 100 µM calcium ionophore (A23187, C7522 Sigma-Aldrich) in Sage cleavage + 10% HSA (Cooper Surgical, USA) from a stock solution in DMSO (Sigma-Aldrich) diluted 1:40. Oocytes were transferred to 35 µl drops of the activation medium under Sage oil, numbered appropriately. Activation culture was performed for 40-120 mins. The oocytes were then moved to post activation culture.

Post activation culture was performed in separate wells of EmbryoScope slides (Unisence Fertilitech, Denmark) in cleavage medium - medium as used in post warm culture under Sage oil. The slides were placed in the EmbryoScope time lapse incubator (Unisence Fertilitech, Denmark) for assessment of second polar body (PB2) extrusion and appearance of pronuclei prior to PB2 biopsy.

Polar body biopsy

Polar bodies were biopsied sequentially in order to discriminate between the 3 products of meiosis using micromanipulators (Narishige, Japan) on an inverted microscope (Nikon Ltd, Japan) equipped with Hoffman Modulation contrast and a 37°C heating stage (Linkam Scientific Instruments, UK). The first polar body (PB1) was biopsied prior to oocyte activation and the second polar body (PB2) was biopsied following its extrusion, post activation as previously described by Capalbo et al.[16]. All biopsies were performed in individually numbered 10 µl microdrops of HEPES medium + 10% HSA under Sage oil (Cooper Surgical, USA) for tractability. For both PB1 and PB2 biopsies, oocytes were positioned on the microscope to give a clear view of the PB and secured by suction with the holding pipette (TPC, Australia). An aperture was made in the zona pelucida with a series of laser pulses (Saturn laser; Research Instruments, UK) working inwards from the outer surface of the zona. The aspiration pipette (zona drilling pipette; TPC, Australia) was then inserted through the opening and the PB removed with gentle suction. PB1 biopsy: Once biopsied the oocytes were moved to activation culture leaving the biopsied PB1 in the microdrop for immediate transfer to a 0.2 ml, RNase and DNase free thin walled, flat cap PCR tube (Corning, Sigma-Aldrich) for DNA amplification. PB2 biopsy: once biopsied the PB2 was immediately transferred to a PCR tube for DNA amplification with the oocyte still in the microdrop. The oocyte was then returned to the micromanipulator for full zona removal. The zonae were removed from the oocytes using the same setup for the biopsy procedure. The oocyte was anchored to the holding pipet and a larger aperture was made in the zona using laser pulses. The oocyte was removed from the zona using both displacement and zona manipulation techniques with the aspiration pipette. Once free from the zonae, the oocytes were transferred to PCR tubes for DNA amplification.

Transfer of the samples to PCR tubes was performed using a plastic denuding pipette (COOK Medical, Ireland) with a 130 µm lumen. Individually labelled PCR tubes were primed with 2 µl Dulbecco's phosphate buffered saline (DPBS) (Gibco, Life technologies) with 0.1% polyvinyl alcohol (Sigma-Aldrich). Individual samples were expelled into the DPBS in around 1 µl of the medium containing the samples, leaving a final volume of no more than 4 µl of medium with the sample in the PCR tubes. The PCR tubes were then briefly centrifuged, snap frozen in liquid nitrogen and stored at -20 °C prior to whole genome amplification.

DNA extraction and Whole Genome Amplification (WGA)

Genomic DNA (gDNA) from all oocyte donors was obtained using buccal cell swabs (Isohelix, Cell Projects Ltd). Extraction of the gDNA from the swabs was performed using a proteinase K extraction kit to a final volume of 30 µl, following the manufacturer's instructions. DNA from all three products of meiosis was obtained by lysis of the cells and whole-genome amplication (WGA). The PCR tubes containing the samples were brought to an end volume of 4 µl with PBS and REPLI-g Single Cell Kit multiple displacement amplification (SureMDA, Illumina) or PCR library based SurePlex amplification (Illumina) was performed according to the manufacturer's instructions. MDA was performed with a short 2h incubation.

Embryos and embryo-PB trios

Embryo samples

Thirty five embryos diagnosed as affected and/or aneuploid were analysed from four clinical cases for either preimplantation genetic diagnosis (PGD) of single gene defects or preimplantation genetic screening (PGS) for aneuploidy following standard IVF protocols at

The Bridge Centre, London with patients informed consent. SNP genotyping was performed for quality control purposes following clinical biopsy and genetic testing of the embryos under the HFEA clinic licence L0070-14-a using similar methods to those described for the processing of the oocyte-PB trios.

In one of the PGD cases, two surplus denuded MI oocytes were allowed to mature *in vitro* by overnight culture in Sage fertilisation medium +10% HSA under mineral oil (Cooper Surgical). Biopsy of PB1, tubing and WGA of the oocyte and PB1 were then performed as described for the oocyte-PB trios.

Embryo-PB trios

In another PGS case, in which array CGH had been used to detect aneuploidy by copy number analysis of both polar bodies, the WGA products (Sureplex; Illumina, San Diego, CA, USA) from both polar bodies were SNP genotyped along with parental genomic DNAs and, with patients informed consent, WGA products (SureMDA; Illumina, San Diego, CA, USA) of nine corresponding fertilised embryos which had all been diagnosed as aneuploid.

Array CGH, SNP bead array and data analysis

For array CGH analysis, 4 µl aliquots of Sureplex single cell amplified DNA Products (PB1, PB2, oocyte or blastomere) were processed on microarray slides (24Sure; Illumina, USA). The data was imported and analysed using dedicated softwaresoftware (BlueFuse Multi v 4.0; Illumina, USA).

For SNP genotyping, 400 ng of genomic DNA or 8 µl of WGA products from the single cell and embryo samples (PB1, PB2, oocyte, single blastomere or whole embryo) were processed on a SNP genotyping beadarray (Human CytoSNP-12 or Human Karyomapping beadarray; Illumina, San Diego, CA, USA) for ~300K SNPs, using a shortened protocol and

the genotype data analysed using a dedicated software programme for karyomapping (Bluefuse Multi v 4.0; Illumina, San Diego, CA, USA) or exported as a text file for analysis in Micrsoft Excel[12].

MeioMap analysis

Following SNP genotyping, MeioMaps were constructed and displayed by importing the data into Microscoft Excel and processing using custom macros written in Visual Basic for Applications. For the oocyte-PB trios, a simple algorithm was used to phase all heterozygous maternal SNP loci using a haploid PB2 or oocyte sample as a reference. This defined a reference set of homozygous SNP loci (haplotype) genome wide (AA or BB), across each chromosome. The genotype of each of the samples including the reference were then interrogated at each of these informative SNP loci and displayed as either the same as the reference (yellow) or opposite to the reference (green) or heterozygous (blue) indicating the presence of both maternal haplotypes. Phase transitions at crossovers were then manually tagged in Excel by copying the closest SNP calls bracketing the crossover and the type and position of these SNPs imported into a second spreadsheet for further processing. Because phasing is achieved using a reference sample, any phase transitions caused by crossovers in that particular sample appear in identical positions in all other samples analysed (with the exception of any crossover between the reference and the PB2 or oocyte in that trio). Macros in the second spreadsheet therefore identified these common crossovers, restored them to the reference sample and removed them from all of the other samples. The meiomaps were then displayed, checked and further edited manually as necessary. All oocyte-PB trios were run with at least two references to MeioMap any aneuploid chromosomes in the reference trio and to double-check all crossovers.

For embryo-PB trios, two methods were used. Where the SNP genotype of a close relative or, in some cases, a sibling embryo was available, the samples were karyomapped using the standard algorithm which identifies informative SNP loci for all four parental haplotypes in either Excel or using dedicated software (Bluefuse Multi v 4.0; Illumina, San Diego, CA) [11,12]. Alternatively to improve resolution, a modified karyomapping algorithm, with a PB2 or oocyte as reference, was used. This algorithm identified all combinations of parental genotypes that were informative for the maternal haplotype only. In either case, the phase transitions were manually tagged and imported into the second spreadsheet for further processing, display and final editing as above.

We validated our workflow on single cells by comparing recombination maps in 15 individual cells from a donor to the genomic DNA of the child, and by assessing 10 individual blastomeres from the same embryo for direct comparison. In all cases, concordance of recombination rates and positions was >99% (data not shown).

Simulation: crossover distribution amongst chromosomes and distances between crossovers along chromosomes.

12% of crossovers occurred between the PB2 and oocyte and a similar proportion would be expected to occur in the PB1, which go undetected since the heterozygous SNPs (blue regions) cannot be phased.

Maternal recombination rates in the oocyte-PB and embryo-PB trios were similar to those reported from foetal oocytes[28-30] as well as female pronucleus-PB trios from young women[10]. When only the embryo or oocyte was used, >50% of crossovers went undetected in the two polar bodies (Fig.3a-b) . The recombination rates in the oocyte or embryo correlated well with those discerned from polar bodies (Extended Data Figure S3). This supports the notion that recombination occurs randomly amongst non-sister chromatids. Indeed, when

homolog pairs had engaged in crossing over twice, no evidence of increased or decreased probability of the same two chromatids engaging in the second crossover was detected (Methods). This is consistent with reports that the preference for two sister chromatids to re-engage in a second crossover given their involvement in the first (negative chromatid interference) is very weak[10].

Simulations were performed to allocate a specified number of crossover events to set of chromosomes. Chromosomes were allocated a specified length using the minimum and maximum crossover locations mapped within the experimental dataset. Crossovers were allocated randomly to chromosomes with weighted probability using the chromosome length, thus longer chromosomes receive more crossovers. The allocation was either totally random (non-obligate) or random following allocation of one crossover per chromosome (obligate). For each chromosome the positions of the allocated crossovers was determined iteratively by randomly selecting an available location. The available locations were all possible positions not within a minimum distance (107 kb) from the existing crossover positions. The simulation reported the total number of crossovers per chromosome and the inter-crossover distances. The distance from the outermost crossover to the chromosome termini was not included. 10,000 simulations were performed to create the distributions. The scripts (Ottolini_Scripts_CrossoverData.pl) are freely available under copyright and GNU public licence.

To estimate the fraction of missed crossovers, we randomly distributed 125 crossovers amongst chromosomes with a minimum distance of 0 kb between them (Ottolini_Scripts_CrossoverData.pl). A cumulative distribution of inter-crossover distances was constructed, ignoring crossover distances that were adjacent to telomeres. The cumulative frequencies was 0.04% at 10 kb, 0.15% at 30 kb, 0.52% at 107 kb, 0.75% at 150 kb, and 1% at 200 kb.

Chromatid interference.

To detect chromatid interference, we identified 134 chromosome pairs with two crossovers and we asked whether the same two chromatids were less or more likely to be involved in both crossover events compared to random participation. We were unable to reject the null hypothesis of no chromatid interference ($p > 0.5$; t-test for proportions), consistent with reports that negative chromatid interference is weak [10].

Statistics, modelling, and graphics.

Statistical tests and modelling were carried out in Perl or R. All tests were permutation and non-parametric tests, or logistic regression analysis as indicated throughout the manuscript. For logistic regression, we used the AIC to choose the appropriate link function. Binomial distribution of error variances were assessed using the plot(model) function of R. Residual variance and degrees of freedom was tested using chi-square and rejected if below 5%. Two-sided tests were employed, unless otherwise indicated. We used the lme4, lmPerm, psperman libraries in R. Graphics were rendered using the basic functions in R or the ggplot2 library[54].

Fig.1

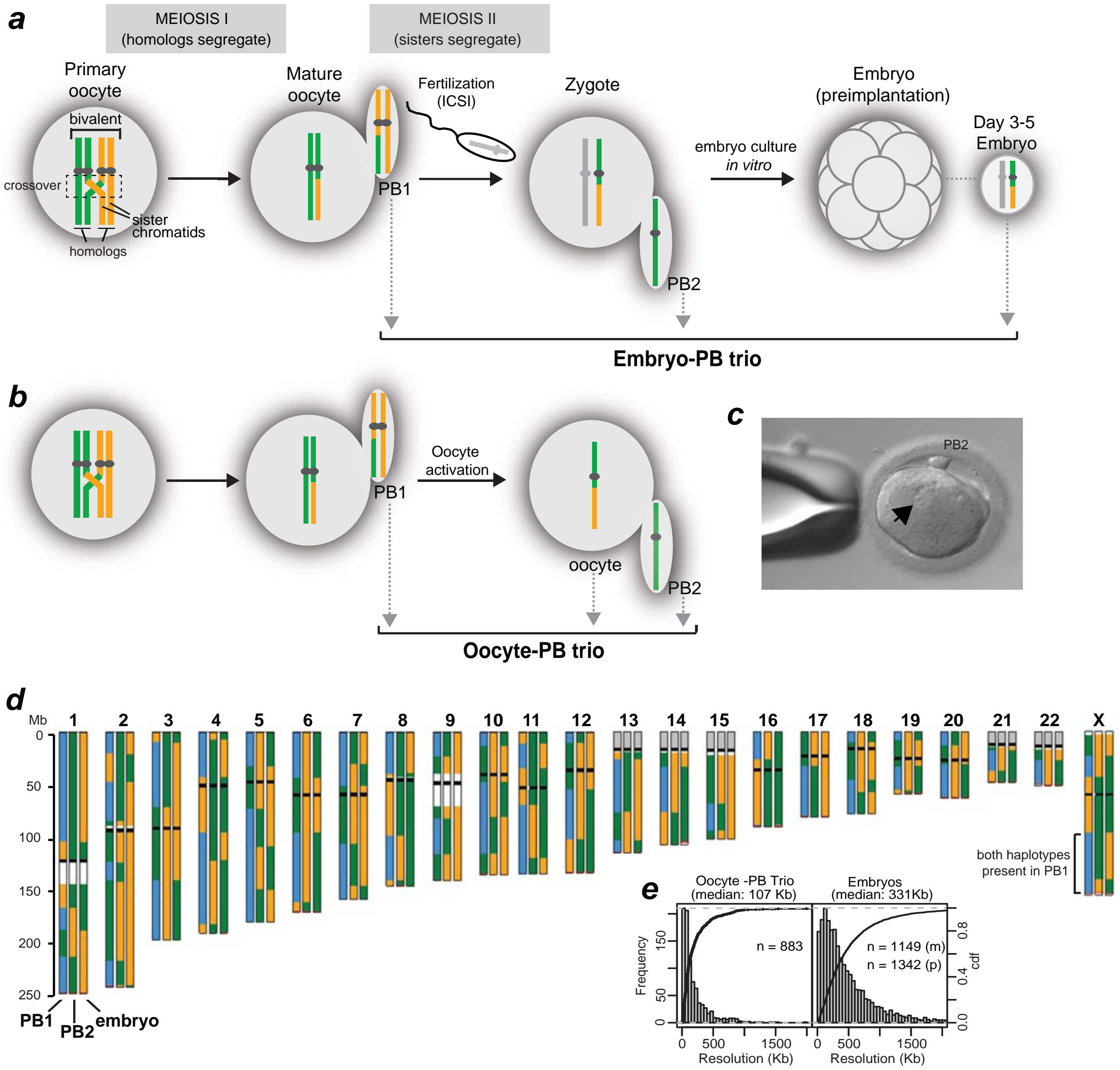

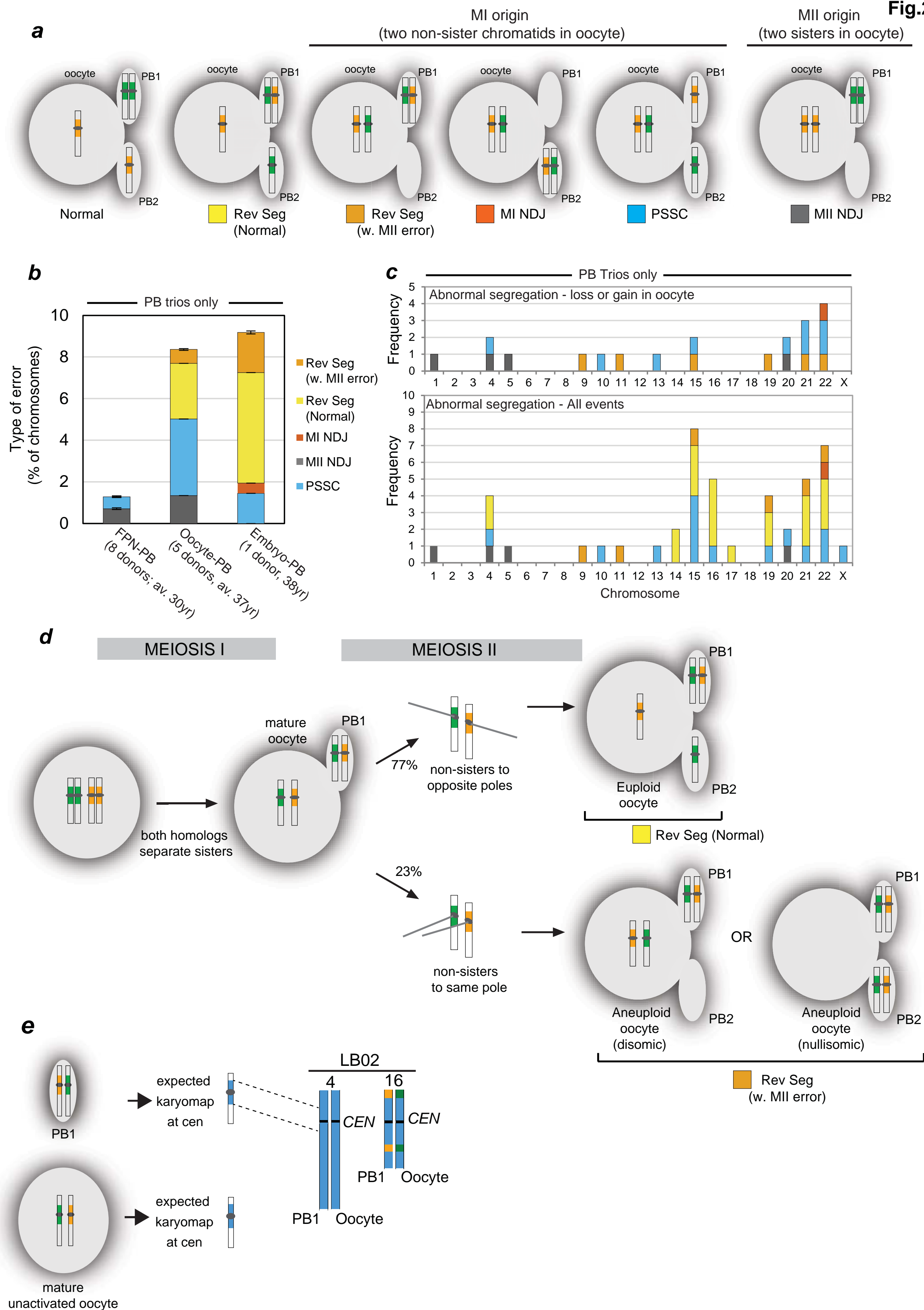

Fig.2
a
MI origin
(two non-sister chromatids in oocyte)
MII origin
(two sisters in oocyte)
oocyte
PB1
PB2
Normal
Rev Seg
(Normal)
Rev Seg
(w. MII error)
MI NDJ
PSSC
MII NDJ
b
PB trios only
Type of error
(% of chromosomes)
Rev Seg
(w. MII error)
Rev Seg
(Normal)
MI NDJ
MII NDJ
PSSC
FPN-PB
(8 donors; av. 30yr)
Oocyte-PB
(5 donors, av. 37yr)
Embryo-PB
(1 donor, 38yr)
c
PB Trios only
Abnormal segregation - loss or gain in oocyte
Abnormal segregation - All events
Frequency
Chromosome
d
MEIOSIS I
MEIOSIS II
both homologs
separate sisters
mature
oocyte
77%
non-sisters to
opposite poles
Euploid
oocyte
Rev Seg (Normal)
23%
non-sisters
to same pole
OR
Aneuploid
oocyte
(disomic)
Aneuploid
oocyte
(nullisomic)
Rev Seg
(w. MII error)
e
expected
karyomap
at cen
LB02
CEN
PB1
Oocyte
mature
unactivated oocyte

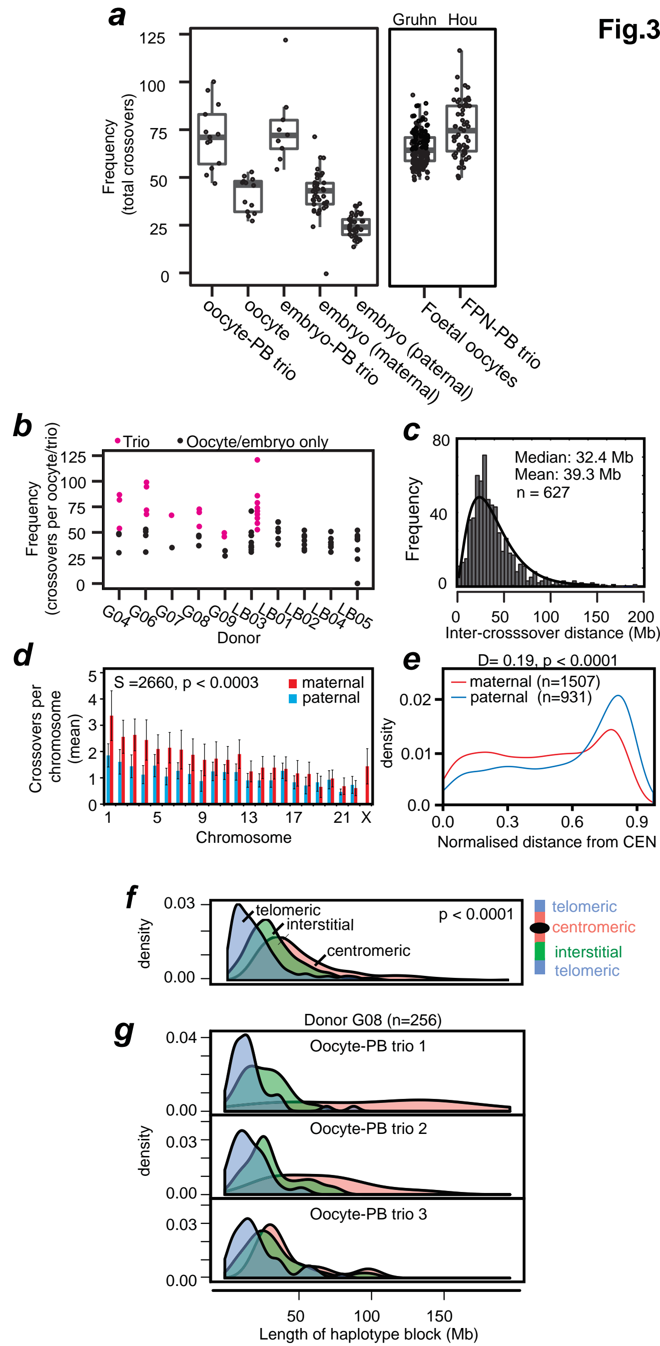
Fig.3
a
Frequency (total crossovers)
Gruhn
Hou
oocyte-PB trio
oocyte
embryo-PB trio
embryo (maternal)
embryo (paternal)
Foetal oocytes
FPN-PB trio
b
Trio
Oocyte/embryo only
Frequency (crossovers per oocyte/trio)
Donor
c
Median: 32.4 Mb
Mean: 39.3 Mb
n = 627
Frequency
Inter-crosssover distance (Mb)
d
S =2660, p < 0.0003
maternal
paternal
Crossovers per chromosome (mean)
Chromosome
e
D= 0.19, p < 0.0001
maternal (n=1507)
paternal (n=931)
density
Normalised distance from CEN
f
telomeric
interstitial
centromeric
p < 0.0001
density
g
Donor G08 (n=256)
Oocyte-PB trio 1
Oocyte-PB trio 2
Oocyte-PB trio 3
density
Length of haplotype block (Mb)

Fig. 4

a

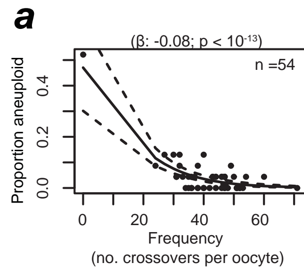

b

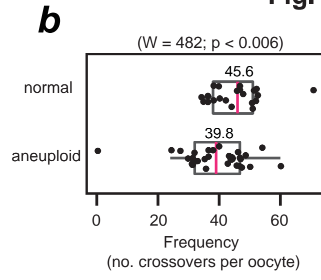

c

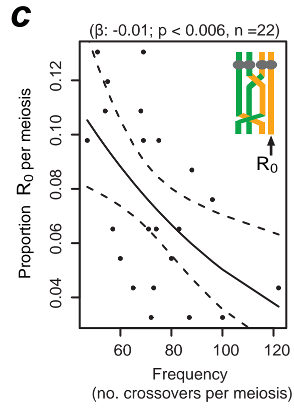

d

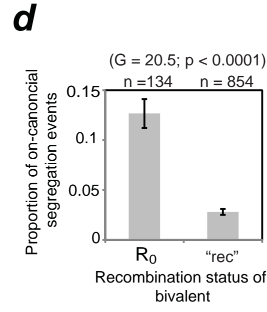

Fig.5

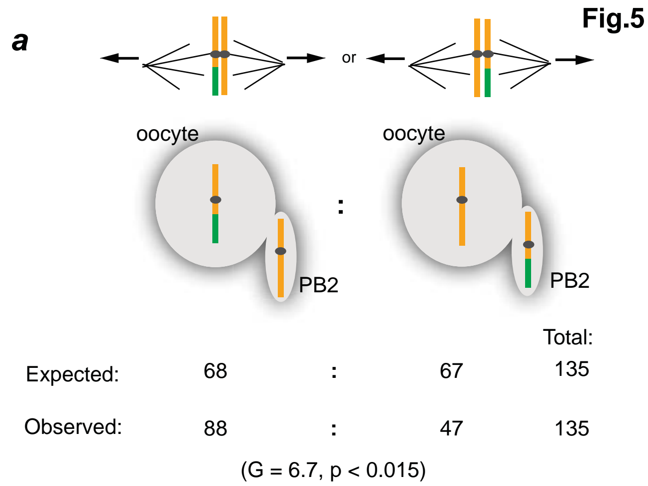

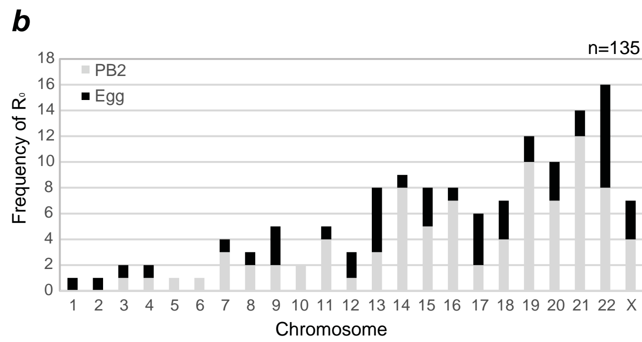

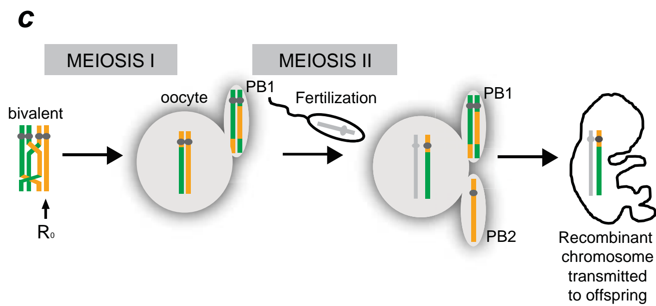

Fig. S1

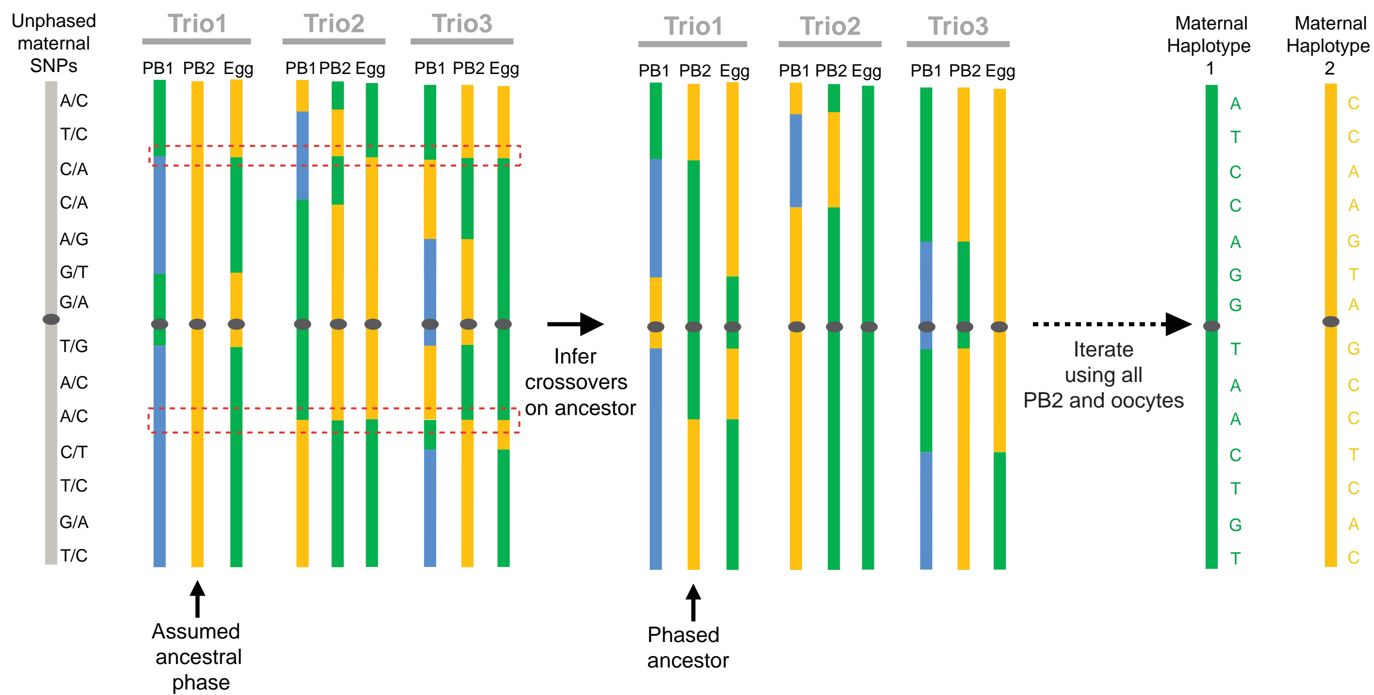

Fig. S2

G04_Trio 1

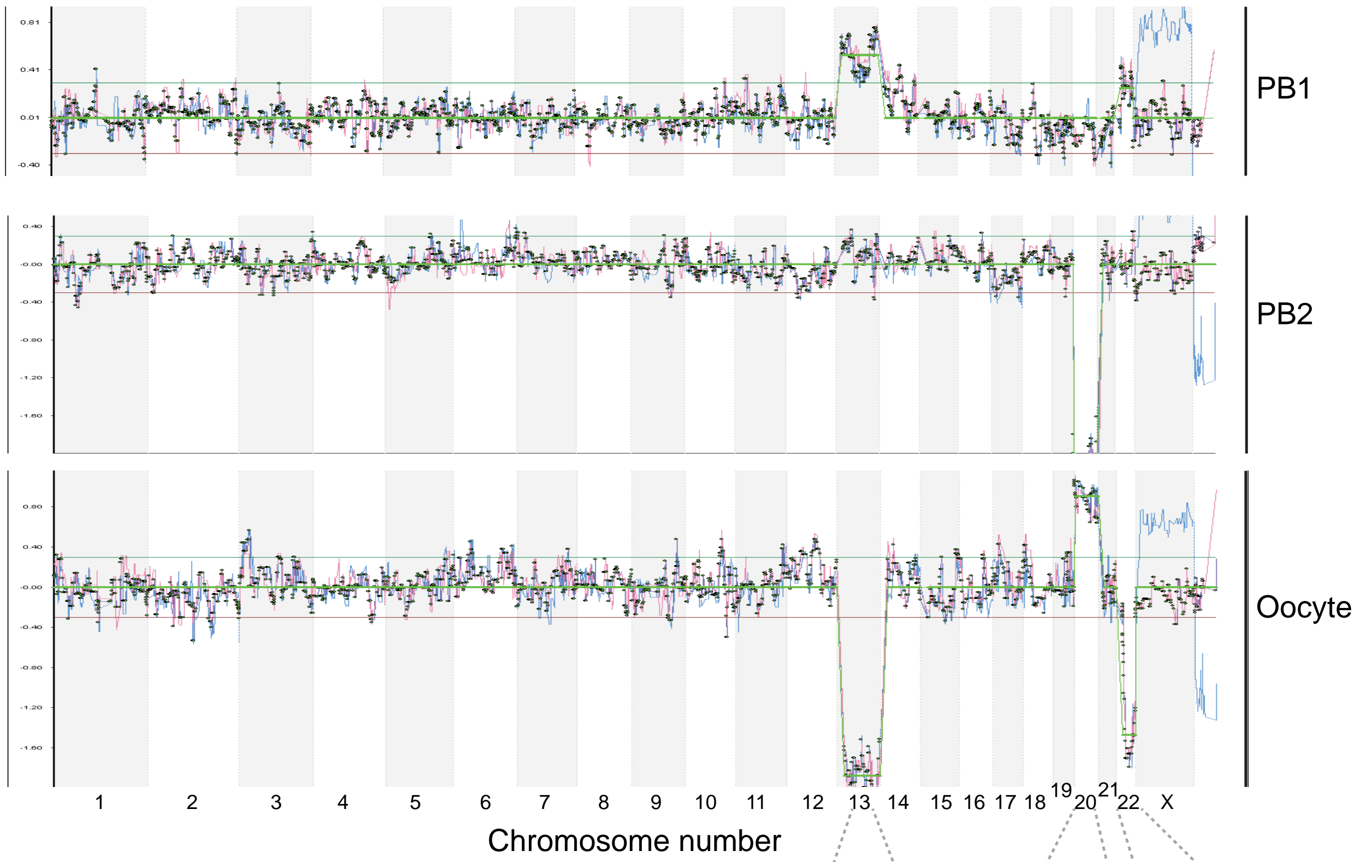

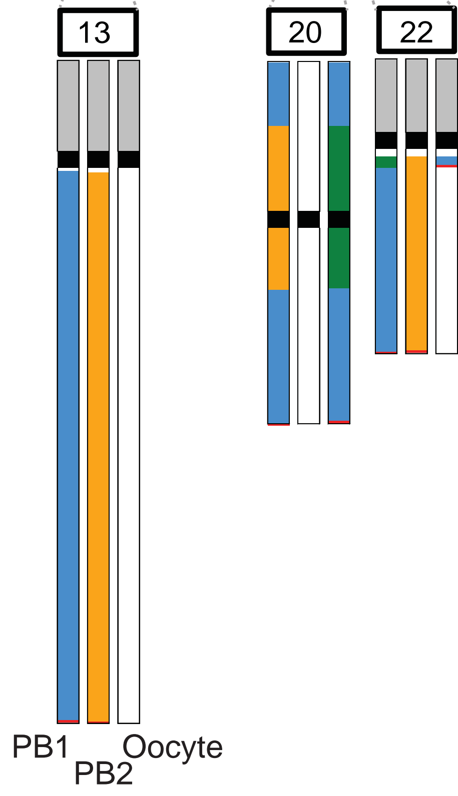

Fig. S3

a Meiosis I nondisjunction:

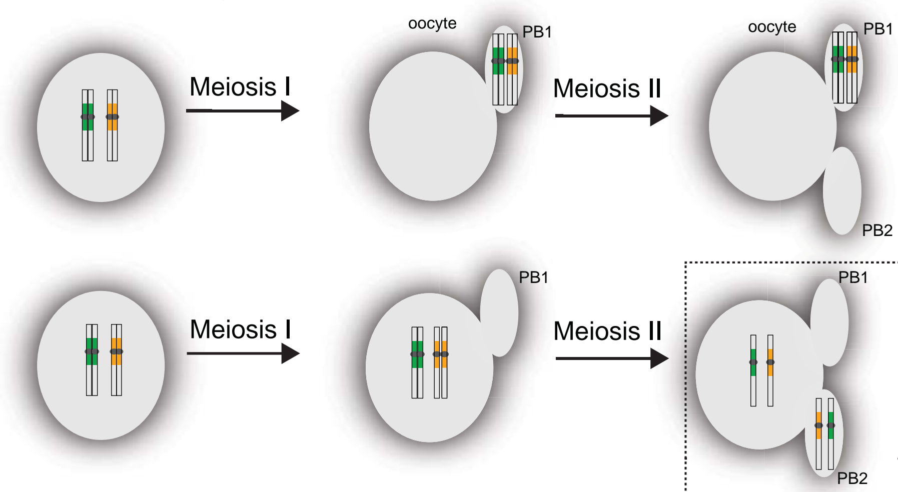

b Precocious separation of sister chromatids (PSSC):

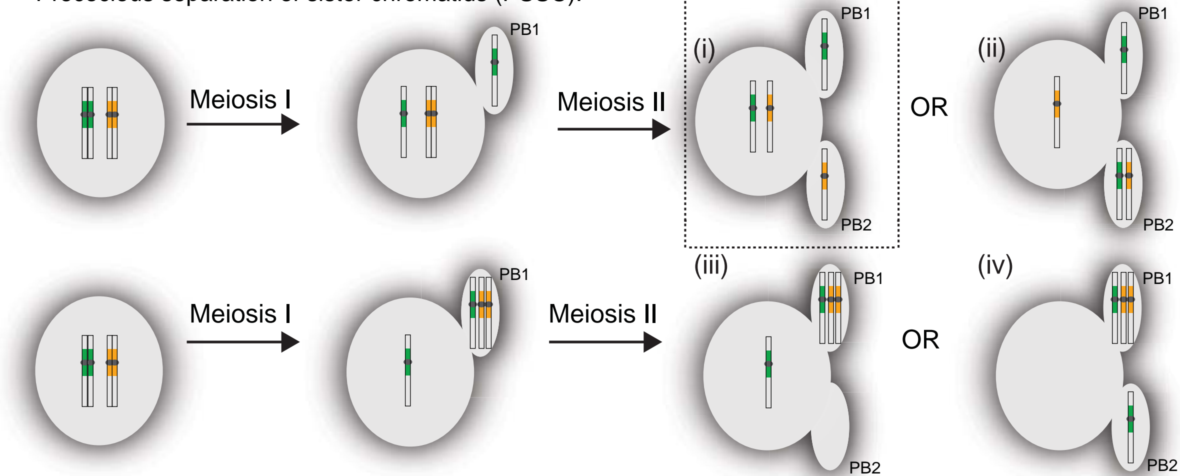

c MII nondisjunction or PSSC with normal MI segregation:

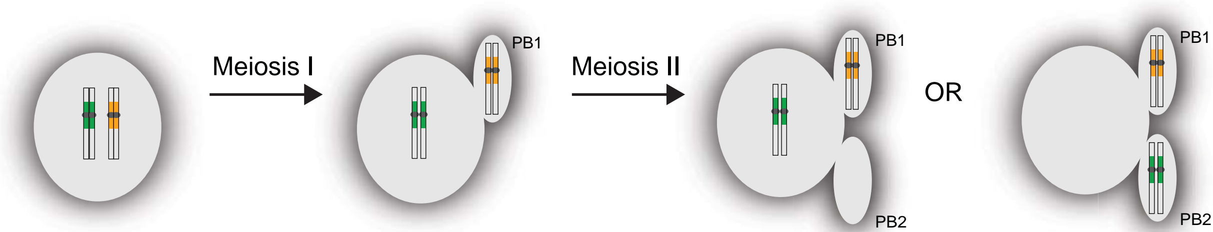

d Reverse segregation (Rev Seg):

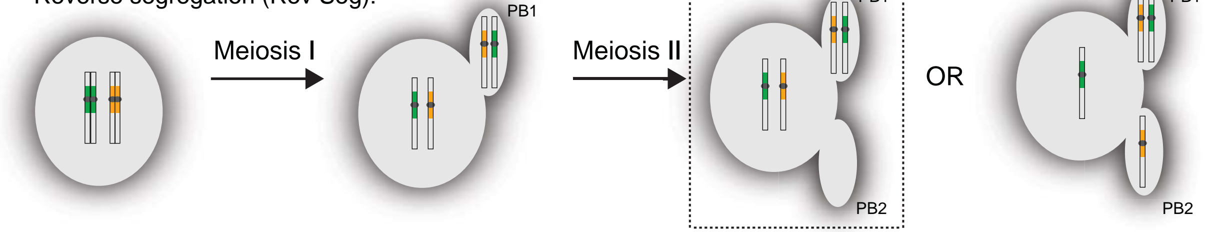

Fig. S4

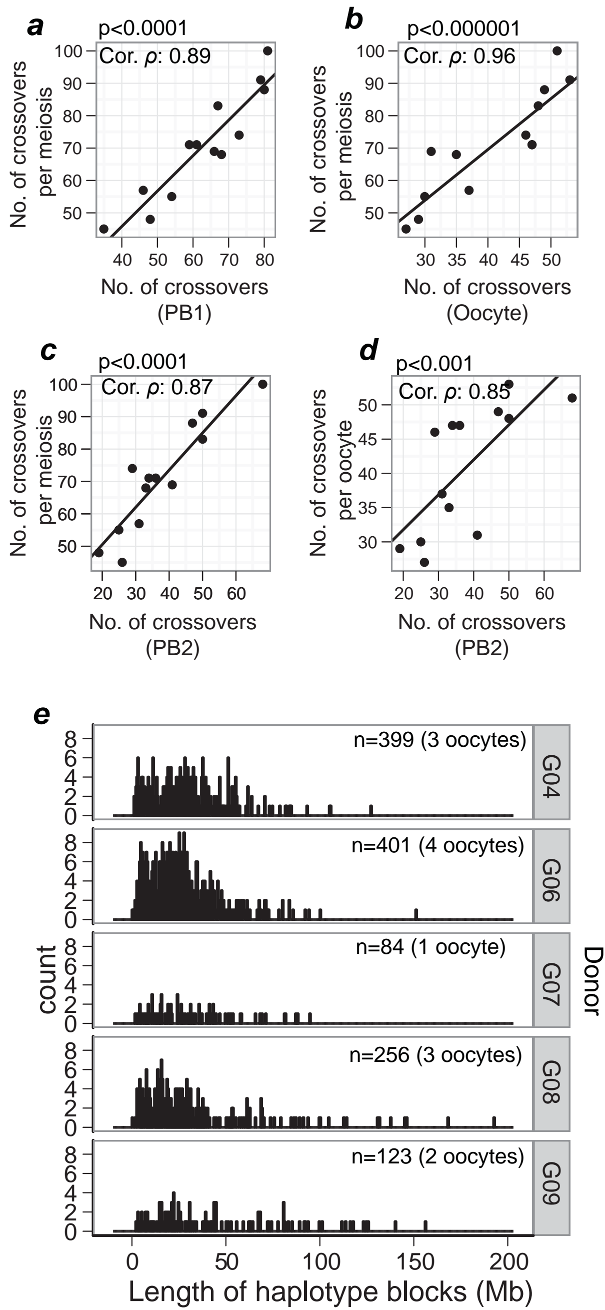

Fig. S5

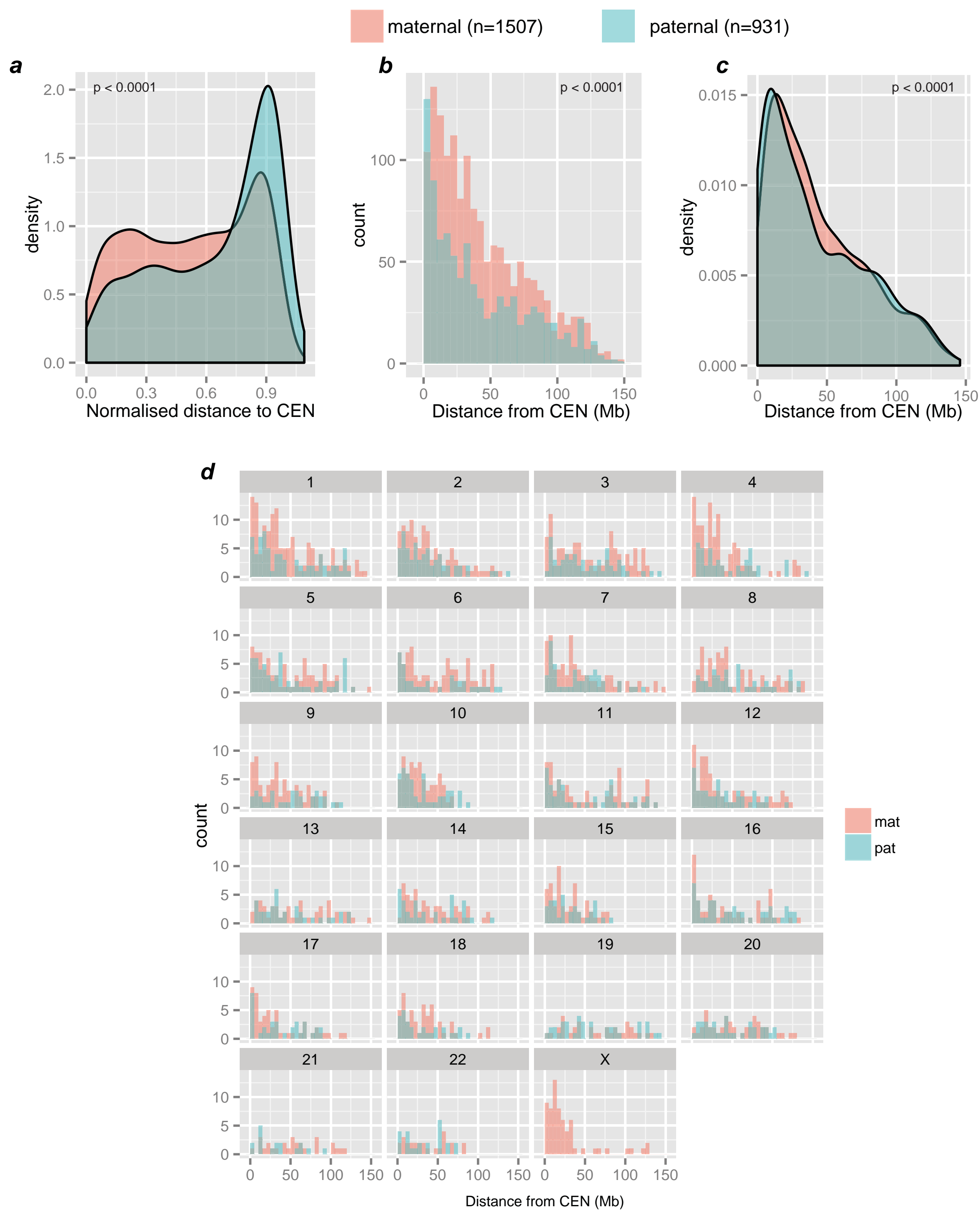

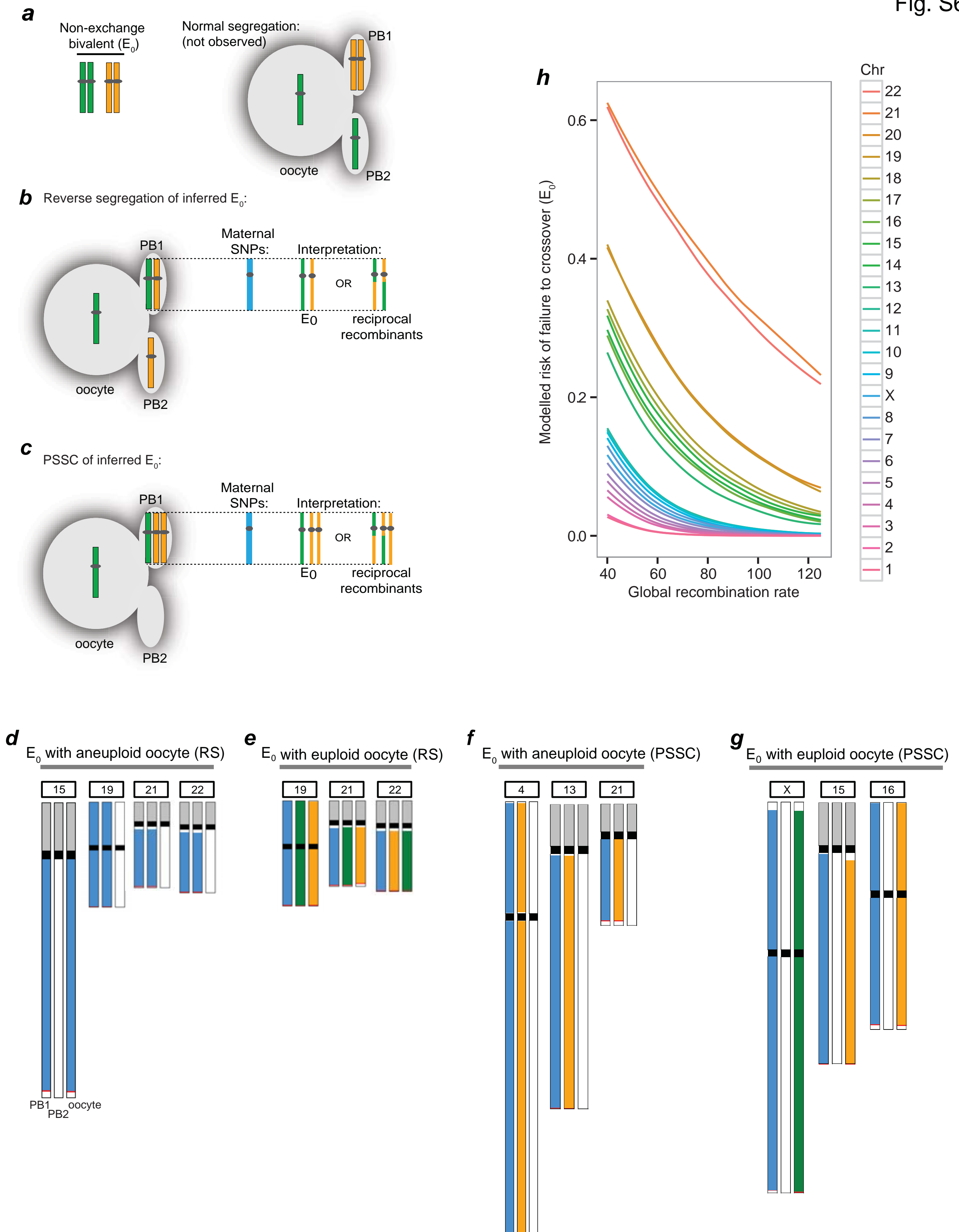
a
Non-exchange bivalent (E_0)
Normal segregation: (not observed)
PB1
PB2
oocyte
b Reverse segregation of inferred E_0:
PB1
Maternal SNPs:
Interpretation:
OR
E0
reciprocal recombinants
oocyte
PB2
c PSSC of inferred E_0:
PB1
Maternal SNPs:
Interpretation:
OR
E0
reciprocal recombinants
oocyte
PB2
h
Modelled risk of failure to crossover (E_0)
0.0
0.2
0.4
0.6
40
60
80
100
120
Global recombination rate
Chr
22
21
20
19
18
17
16
15
14
13
12
11
10
9
X
8
7
6
5
4
3
2
1
d E_0 with aneuploid oocyte (RS)
15
19
21
22
PB1
PB2
oocyte
e E_0 with euploid oocyte (RS)
19
21
22
f E_0 with aneuploid oocyte (PSSC)
4
13
21
g E_0 with euploid oocyte (PSSC)
X
15
16

Extended Data Table 1. Donor information for embryos[a]

Donor ID	Age	Oocytes Retrieved	No. Embryos Analysed	Stage of pre-implantation embryo development			Permission to biopsy PBs	No. Embryos Transferred	Live Birth Outcome	Reason for karyomapping
				Cleavage	Morula	Blastocyst				
LB01	38	8	4	2	1	1	no	1	Live birth	PGD for single gene disorder and PGS for advanced maternal age
LB02	35	10	6	2	0	4	no	2	Twin live birth	PGD for single gene disorder
LB03	38	21	10	5	1	4	9	1	None	PGS for recurrent miscarriage
LB04	34	23	8	5	3	0	no	1	None	PGD for paternal translocation
LB05	41	27	10	10	0	0	no	1	Live Birth	PGS for advanced maternal age
		Total:	**38**				**9**	**5**	**3**	

[a]From The Bridge Centre, UK. Diagnostic follow-up in compliance with the code of practise (HFEA).

[b]Donor of the two MII-arrested oocyte-PB1 duos (see Methods).

[c]Corresponding embryo with both polar bodies analysed for MeioMapping.

[d]embryo giving rise to live births not mapped.

[e]Translocation chromosomes were excluded from the analysis.

Extended Data Table 2. Donor information for oocyte-PB trios

StudyID	oocytes collected	oocytes vitrified	Oocytes used for study	Oocytes after warming	Activated oocytes	Complete trios amplified	Patient age	Pregnancy from cycle	Reason for infertility
G01	10	10	4	4	2	0	37.4	no	idiopathic
G02	6	3	3	3	3	0	36.2	yes	male factor
G03	15	10	10	5	3	0	37.6	yes	male factor
G04*	11	5	5	5	5	3	35.7	no	male factor
G05	11	6	3	3	3	0	37.3	yes	idiopathic
G06*	12	6	6	5	4	4	40.6	yes	male factor
G07*	16	9	6	6	5	1	38.4	yes	tubal
G08*	10	7	5	5	5	3	37.9	yes	endometriosis
G09*	12	fresh	2	2	2	2	33.2	yes	male factor
G10	18	18	3	2	2	0	39.0	no	male factor
			Total:	**40**	**34**	**13**	**37.3**		

*trios used to generate MeioMaps. Average age: 37.2 years.

Extended Data Table S3. Structural rearrangements to chromosomes in meiosis

Donor ID	Chromosome	Breakpoint position (Mb)	Description
G04_1*	22q	18.6 Mb	Loss of large section of q-arm in oocyte, reciprocal gain in PB1
G04_3*	8p	9.6 Mb	Gain of small region at p-Ter in oocyte, reciprocal loss in PB1
G09_2*	15q	44.1 Mb	Gain of region of q-arm in oocyte, reciprocal loss in PB1
LB03_13**	4q	83.07 Mb	Deletion of large region in PB2 only

*from oocyte-PB trios; **from embryo data only (no PB data)

Extended Data Table 4. Summary of recombination and chromosome segregation in all trios.

Oocyte-PB Trios:

Donor	Trio		chromosome 1	2	3	4	5	6	7	8	9	10	11	12	13	14	15	16	17	18	19	20	21	22	X	Total
G04	3	PB1	6	4	4	3	3	2	3	3	3	3	2	2	0	1	1	3	1	1	2	2	1	1	3	54
		PB2	3	1	3	1	1	1	2	1	2	1	1	3	0	0	0	2	0	0	0	n/a	0	0	3	25
		Egg	3	3	1	2	2	1	1	2	1	2	1	1	n/a	1	1	1	1	1	2	2	1	0	0	30
		Total	6	4	4	3	3	2	3	3	3	3	2	3	0	1	1	3	1	1	2	2	1	1	3	55
G04	4	PB1	6	5	4	3	4	4	3	5	4	2	2	3	2	2	0	2	3	3	3	2	1	1	3	67
		PB2	3	2	1	5	4	2	2	2	4	3	3	2	4	1	0	2	3	4	1	0	0	0	2	50
		Egg	5	7	3	4	2	2	1	5	0	1	3	1	2	1	1	0	0	1	2	2	1	1	3	48
		Total	7	7	4	6	5	4	3	6	4	3	4	3	4	2	1	2	3	4	3	2	1	1	4	83
G04	5	PB1	5	6	5	4	4	5	5	3	4	4	3	4	2	2	3	5	3	2	3	2	1	1	4	80
		PB2	3	5	2	4	2	2	0	1	4	3	3	3	4	0	2	2	2	2	0	0	0	0	3	47
		Egg	2	3	3	n/a	2	5	5	4	0	1	0	1	2	2	3	3	1	2	3	2	1	1	3	49
		Total	5	7	5	4	4	6	5	4	4	4	3	4	4	2	4	5	3	3	3	2	1	1	5	88
G06	1	PB1	4	5	4	0	5	7	2	2	5	2	2	4	3	3	2	2	4	2	3	2	2	1	0	66
		PB2	4	5	3	0	3	3	1	3	4	2	0	2	2	0	0	1	3	2	0	1	1	1	n/a	41
		Egg	0	0	1	n/a	2	4	1	1	1	4	2	2	1	3	2	1	1	0	3	1	1	0	0	31
		Total	4	5	4	0	5	7	2	3	5	4	2	4	3	3	2	2	4	2	3	2	2	1	0	69
G06	2	PB1	6	6	5	5	4	5	3	4	4	5	3	3	4	0	3	3	3	2	2	2	1	2	6	81
		PB2	5	6	4	7	6	2	4	4	3	3	1	1	1	1	2	2	2	3	0	3	1	2	5	68
		Egg	3	4	5	2	6	3	5	2	1	2	2	2	3	1	1	1	1	3	2	1	0	0	1	51
		Total	7	8	7	7	8	5	6	5	4	5	3	3	4	1	3	3	3	4	2	3	1	2	6	100
G06	3	PB1	6	8	6	4	5	4	5	2	3	5	3	4	4	3	2	2	5	2	2	2	1	1	5	79
		PB2	5	4	6	4	2	2	4	1	0	5	0	4	1	3	2	0	3	3	1	0	0	0	1	50
		Egg	3	6	4	4	3	4	1	1	3	2	3	4	3	0	2	2	2	1	1	2	1	1	4	53
		Total	7	9	8	6	5	5	5	2	3	6	3	6	4	3	3	2	5	3	2	2	1	1	5	96
G06	4	PB1	5	6	3	2	4	4	3	3	2	2	3	3	3	1	3	3	2	2	0	2	1	2	2	59
		PB2	2	8	1	3	1	2	0	1	1	3	2	1	2	1	1	1	2	1	1	1	0	1	2	36
		Egg	3	4	2	3	3	2	3	2	3	3	1	2	3	2	2	2	0	1	1	3	1	1	0	47
		Total	5	9	3	4	4	4	3	3	3	4	3	3	4	2	3	3	2	2	1	3	1	2	2	73
G07	2	PB1	3	5	7	4	3	5	2	3	4	5	4	2	1	2	0	3	3	2	2	3	2	1	2	68
		PB2	1	3	3	2	2	2	2	2	2	1	3	1	1	0	n/a	0	2	2	0	2	1	1	2	33
		Egg	2	2	4	2	1	3	0	1	2	4	1	1	0	2	0	3	1	0	2	1	1	0	0	35
		Total	3	5	7	4	3	5	2	3	4	5	4	2	1	2	0	3	3	2	2	3	2	1	2	68
G08	1	PB1	3	3	4	0	2	2	2	2	2	3	2	3	1	2	1	3	1	2	2	2	1	1	2	46
		PB2	2	3	1	4	0	1	1	1	1	1	3	2	1	1	3	1	0	1	1	1	1	0	1	31
		Egg	1	2	3	4	2	1	3	1	1	4	1	1	0	1	2	2	1	3	1	1	0	1	1	37
		Total	3	4	4	4	2	2	3	2	2	4	3	3	1	2	3	3	1	3	2	2	1	1	2	57
G08	2	PB1	4	6	5	4	4	2	2	2	3	3	5	2	2	1	0	3	2	2	2	2	1	1	3	61
		PB2	1	3	2	1	3	3	3	1	2	2	2	1	0	1	n/a	0	3	0	0	1	0	1	4	34
		Egg	3	3	3	3	1	5	1	1	3	1	3	3	2	2	0	3	1	2	2	1	1	2	1	47
		Total	4	6	5	4	4	5	3	2	4	3	5	3	2	2	0	3	3	2	2	2	1	2	4	71
G08	3	PB1	5	2	7	4	6	4	2	2	5	3	3	4	4	2	3	3	3	2	2	2	2	1	2	73
		PB2	n/a	2	3	1	3	1	1	0	3	2	0	2	3	0	1	1	2	1	0	1	1	1	0	29
		Egg	5	2	4	3	3	3	1	2	2	1	3	2	1	2	2	2	1	1	2	1	1	0	2	46
		Total	5	3	7	4	6	4	2	2	5	3	3	4	4	2	3	3	3	2	2	2	2	1	2	74
G09	1	PB1	3	2	3	2	3	2	2	2	2	0	2	1	3	3	1	0	1	1	1	0	1	1	1	37
		PB2	2	2	3	2	3	1	0	1	1	1	2	0	2	1	2	n/a	1	0	1	1	1	1	0	28
		Egg	3	2	2	2	n/a	1	2	1	1	n/a	0	1	2	3	3	0	0	1	0	1	0	0	1	26
		Total	4	3	4	3	3	2	2	2	2	1	2	1	4	4	3	0	1	1	1	1	1	1	1	47
G09	2	PB1	3	4	2	2	5	3	3	2	4	2	3	3	1	1	1	1	2	2	1	3	0	1	2	51
		PB2	1	2	0	1	1	1	2	0	2	0	n/a	1	1	0	0	0	1	1	0	3	0	1	1	19
		Egg	2	2	2	1	4	2	1	2	2	2	3	2	0	1	1	1	1	1	1	0	n/a	0	1	32
		Total	3	4	2	2	5	3	3	2	4	2	3	3	1	1	1	1	2	2	1	3	0	1	2	51

PSSC-aneuploid | MI NDJ | MII NDJ | RS-aneuploid | RS-euploid | PSSC-Euploid

Embryo-PB Trios:

Donor	Trio		chromosome																						Total
			1	2	3	4	5	6	7	8	9	10	11	12	13	14	15	16	17	18	19	20	21	22	X	
LB03	2	PB1	4	6	3	3	2	3	2	3	3	3	3	3	3	2	2	2	1	2	3	2	2	1	3	61
		PB2	2	5	1	3	3	1	3	2	3	2	2	2	1	1	2	1	1	1	1	1	1	0	2	41
		Embryo	2	3	2	4	3	2	3	1	0	3	3	1	2	1	0	1	0	3	2	1	1	1	3	42
		Total	4	7	3	5	4	3	4	3	3	4	4	3	3	2	2	2	1	3	3	2	2	1	4	72
LB03	7	PB1	5	2	3	3	3	3	2	2	2	2	3	2	2	1	1	2	3	2	2	3	1	1	2	52
		PB2	2	2	2	1	2	0	1	3	0	2	2	2	1	2	1	0	1	1	1	2	0	1	0	29
		Embryo	3	2	3	2	3	3	1	1	2	2	1	2	1	1	2	2	2	1	1	1	1	0	2	39
		Total	5	3	4	3	4	3	2	3	2	3	3	3	2	2	2	2	3	2	2	3	1	1	2	60
LB03	8	PB1	7	7	4	4	6	5	4	5	3	2	2	4	3	2	n/a	3	5	3	2	2	1	2	2	78
		PB2	4	3	2	4	3	2	2	1	0	3	1	4	1	0	n/a	1	2	2	1	0	0	1	3	40
		Embryo	3	4	2	2	3	3	2	4	3	3	1	2	2	2	3	2	3	1	1	2	1	1	3	53
		Total	7	7	4	5	6	5	4	5	3	4	2	5	3	2	3	3	5	3	2	2	1	2	4	87
LB03	10	PB1	4	4	4	5	2	5	2	4	5	2	3	3	2	2	1	0	4	2	0	2	2	1	6	65
		PB2	4	3	2	3	3	4	4	5	1	1	1	4	1	2	3	1	2	2	0	0	3	1	3	53
		Embryo	2	1	4	2	3	1	4	1	4	1	2	1	1	2	2	1	2	2	0	2	1	0	3	42
		Total	5	4	5	5	4	5	5	5	5	2	3	4	2	3	3	1	4	3	0	2	3	1	6	80
LB03	11	PB1	2	5	3	4	3	3	2	4	2	3	3	2	2	1	2	2	3	2	2	2	1	n/a	2	55
		PB2	2	3	1	1	4	2	2	4	1	3	1	2	2	2	1	0	2	2	1	1	1	1	1	40
		Embryo	2	2	4	3	1	1	2	0	1	2	2	2	0	3	1	2	1	0	1	1	2	1	1	35
		Total	3	5	4	4	4	3	3	4	2	4	3	3	2	3	2	2	3	2	2	2	2	1	2	65
LB03	12	PB1	9	10	6	6	9	5	5	7	5	5	5	6	1	2	3	4	3	3	2	3	2	1	3	105
		PB2	5	6	5	3	4	2	2	3	4	4	3	6	1	4	2	1	2	1	3	3	0	0	3	67
		Embryo	4	4	5	5	5	3	7	4	7	3	2	4	0	2	3	3	1	4	1	0	2	1	2	72
		Total	9	10	8	7	9	5	7	7	8	6	5	8	1	4	4	4	3	4	3	3	2	1	4	122
LB03	13	PB1	3	3	2	2	2	3	3	2	2	2	2	2	3	1	1	2	2	2	2	2	0	0	2	45
		PB2	3	2	2	1	1	1	2	1	1	0	0	2	2	3	2	1	1	2	0	0	0	0	3	30
		Embryo	2	3	0	1	3	2	1	1	3	2	2	0	1	2	1	1	1	2	2	2	0	0	1	33
		Total	4	4	2	2	3	3	3	2	3	2	2	2	3	3	2	2	2	3	2	2	0	0	3	54
LB03	14	PB1	5	3	3	4	5	5	5	2	2	3	2	3	3	3	1	4	1	3	0	2	1	0	3	63
		PB2	1	4	3	1	2	4	4	1	3	1	3	2	0	0	0	3	2	1	0	2	0	0	4	41
		Embryo	4	5	2	3	3	1	3	1	1	2	3	3	3	3	1	3	1	2	0	0	1	0	1	46
		Total	5	6	4	4	5	5	6	2	3	3	4	4	3	3	1	5	2	3	0	2	1	0	4	75
LB03	16	PB1	7	2	5	2	4	3	5	4	3	2	3	2	2	3	3	3	2	2	2	2	0	1	2	64
		PB2	6	2	2	2	2	3	2	3	2	1	1	2	1	1	0	2	2	0	2	0	0	1	2	39
		Embryo	3	2	3	0	2	2	3	1	1	1	2	2	1	2	3	1	2	2	0	2	0	0	0	35
		Total	8	3	5	2	4	4	5	4	3	2	3	3	2	3	3	3	3	2	2	2	0	1	2	69

PSSC-aneuploid	MI NDJ	MII NDJ	RS-aneuploid	RS-euploid	PSSC-Euploid